AD-A071 657 ATOMIC ENERGY RESEARCH ESTABLISHMENT HARWELL (ENGLAND) F/G 11/6
ACOUSTIC EMISSION FOR THE PHYSICAL EXAMINATION OF METALS,(U)
JAN 79 H N WADLEY, C B SCRUBY, J H SPEAKE

UNCLASSIFIED AERE-R-9335 NL

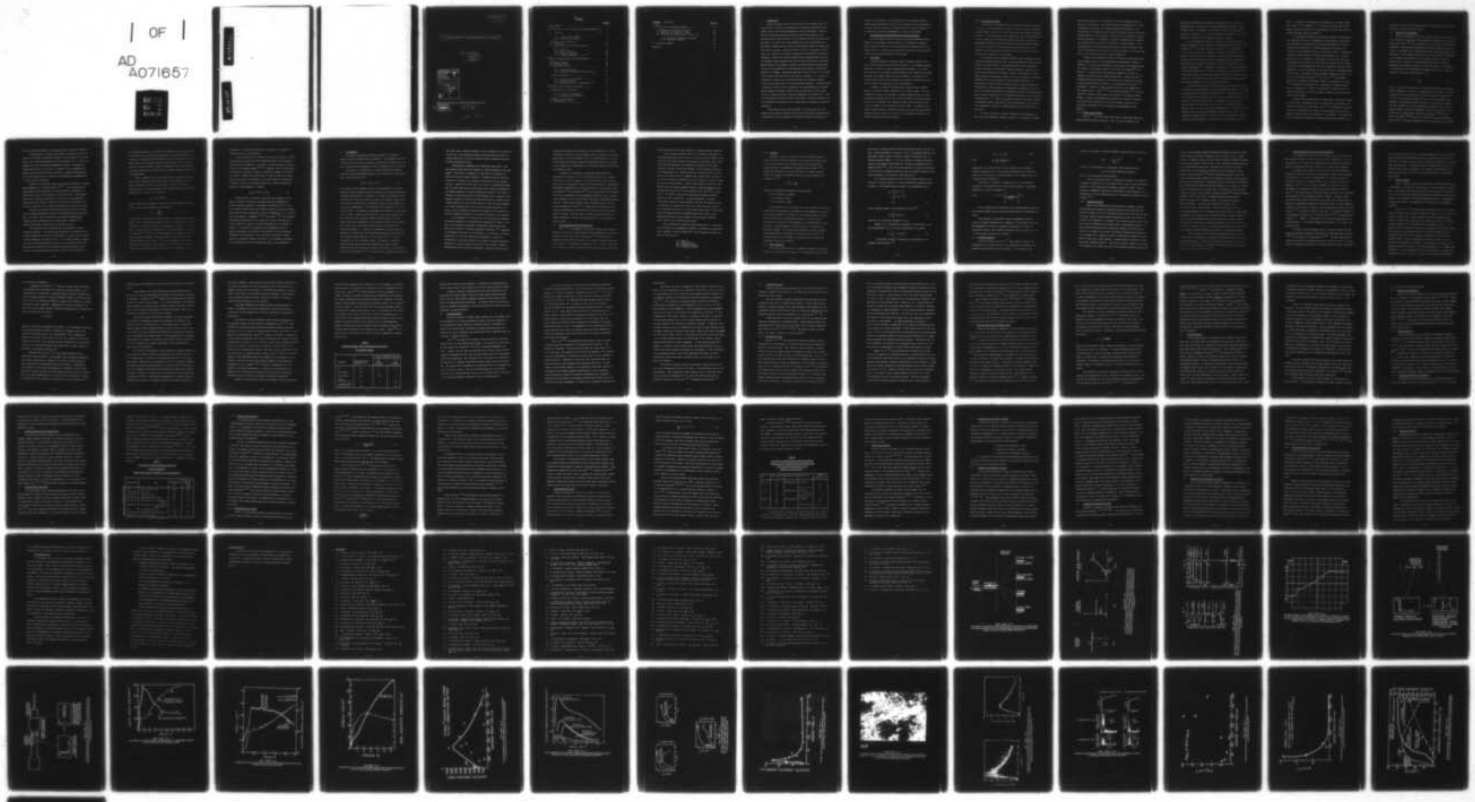

END
DATE FILMED
8-79
DDC

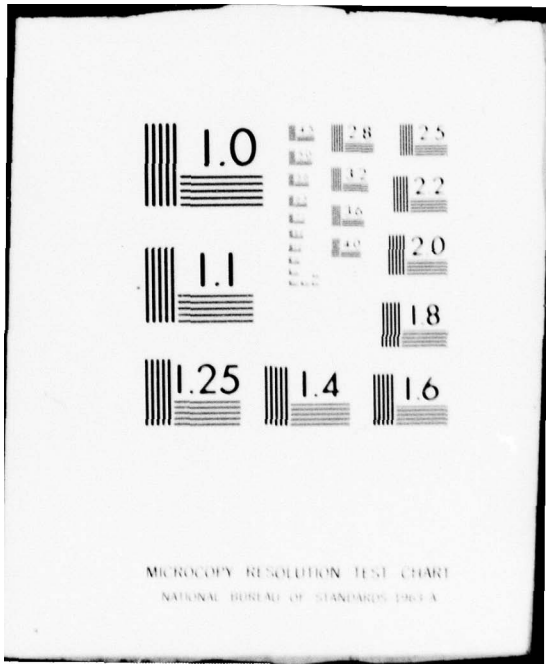
1.0
1.1
1.25
1.4
1.6
2.8
2.5
2.2
2.0
1.8
MICROCOPY RESOLUTION TEST CHART
NATIONAL BUREAU OF STANDARDS 1963-A

(14) AERE-R9335
HL79/362

(6) # ACOUSTIC EMISSION FOR THE PHYSICAL EXAMINATION OF METALS

(10) H. N. G. Wadley*
C. B. Scruby+
J. H. Speake+

Atomic Energy Research Est.
*Metallurgy Division and +Materials Physics Division,
AERE Harwell.

(11) Jan[redacted]1979
(12) 82p.
HL79/362 (C.14)

046 500

CONTENTS

Contents Continued/..

1. Introduction

Acoustic emission is the name given both to the elastic waves generated within a solid as a consequence of deformation and fracture processes, and to the techniques employed for their measurement. Acoustic emission from metals has been studied for some thirty years now, but serious interest and development of the technique did not take place until the 1960's. At that time it was heralded as the most significant test technique to appear for many years, and extravagant claims were made about its ability to detect, locate and identify flaws in structures, and also about its potential for studying the dynamics of deformation and fracture processes. Some of this earlier optimism has subsequently been shown to be unfounded, partly because very little attention was paid to the fundamental aspects of the emission process, and also because the qualitative nature of the measurements has made results from different workers very difficult to compare. Commercial pressures to obtain results in the field on full scale structures must be held partly responsible for the lack of fundamental studies, but it is also true that the necessary wideband recording facilities have only recently become available. In recent years, an increasing effort has been devoted to the understanding of the fundamental aspects of acoustic emission, such as the nature of the source, the way in which the elastic waves are propagated and detected etc. Thus, it is an opportune moment to review the subject of acoustic emission, both as a laboratory instrument and as a viable means of monitoring structural integrity.

This review has four major sections: the first deals with the nature of the acoustic emission source, and the problems of detection and interpretation after propagation of the signal through the material of

interest to the detector; the second deals with the emission arising during plastic deformation; the third with emission from the propagation of cracks; and the fourth with the application of acoustic emission to the detection, location and assessment of flaws in structures.

2. The Detection and Interpretation of Acoustic Emission

In this chapter we shall highlight the limited theoretical understanding of the emission source function, the propagation of elastic waves through the specimen, and the detection and interpretation of the emission signals. We shall also discuss the practical problems inherent in many of the techniques currently being used.

2.1 The Source

Acoustic emission is generated during transient changes in the local stress and strain fields within a material. Such changes accompany deformation, fracture or phase transformation processes. It is hoped that analysis of the acoustic emission waveforms will provide new information about the dynamic features of such processes. The energy of the coherent elastic waves which constitute the emission waveform comes from the work done by the external load on the testpiece.

A number of attempts have been made to model acoustic emission sources, and can be broadly classified in two general types. One type considers the source as a generator of elastic radiation energy and uses macroscopic parameters such as bulk stress and strain to obtain a static solution to the problem. This approach ignores how the source relaxations are related to the deformation process itself. The other, and in many ways more difficult, approach involves using the local time-varying stress and strain fields in the vicinity of the source to calculate the dynamic changes as the source operates.

2.1.1 Static Source Models

This approach considers an energy partition process at the source [1], Fig 1. The stored energy, available within a source for generating coherent elastic waves, is not totally converted into acoustic emission radiation: some is converted into surface energy (due to the creation of new crack faces and/or surface slip steps), some into the energy of a dislocation network and some into heat as a result of plastic deformation. Only a fraction of the available energy is radiated away as transient elastic waves which constitute acoustic emission, and which ultimately are converted to heat energy.

If the energy of the acoustic emission could be measured and the partition function determined, then it might be possible to estimate the energy of the source event. This would provide a means of relating fracture mechanics to microscopic fracture processes. However, this proves rather difficult in practice. Firstly, the fraction of stored energy radiated away depends critically both on the nature of the source mechanism and on the properties of the surrounding material. In particular, the rate of energy release can have a great influence upon the partition of energy amongst the dissipative processes, ie if it is rapid, the material surrounding the emission source may have insufficient time to absorb the energy, and so a substantial fraction may be radiated as elastic waves [2]. Thus, the partition function is itself a variable for different sources, and unless it can be determined for each source it is impossible to relate the radiated energy to the total energy of the source.

A second, and equally important drawback to this approach, is that even if the partition function were known, the fraction of elastic

wave energy impinging on the transducer could vary depending upon the position of the source. This arises because wave propagation in a metal is dispersive and subject to frequency-dependent attenuation. The introduction of surfaces can also change the effective source to detector distance making it very difficult to account for the effects of attenuation and dispersion. In addition, the energy radiated away in a specified direction from the source is a function of source geometry. Thus, the proportion of the emitted energy actually reaching the sensor (and thus the estimated source energy) is a complex function of the configuration of the source, test-piece and sensor properties.

Despite these drawbacks a number of authors have developed static source models to explain their experimental measurements: James and Carpenter [3] consider the breakaway of dislocations from pinning points as a model of the emission source in LiF, whilst both Pascual [4] and Sedgwick [5] consider the multiplication processes as the source in aluminium alloys and alkali halides respectively. Fisher and Lally [6] consider individual co-operative slip events as the source, and attempt to estimate dislocation velocities. Both Kiesewetter and Schiller [7] and Mason [8] attempt to relate acoustic emission to the operation of Frank-Read sources. Gillis [9,10] and Gillis and Hamstad [11] have discussed the relation between dislocation motion and the energy release process. However, the quantitative relationships required to provide a new insight into deformation and fracture processes have yet to be calculated, principally for the reasons already discussed in this section.

2.1.2 Dynamic Source Models

Pollock [12] has developed a more dynamic source model based on a mass supported between two springs. When the spring constant of one

spring was instantaneously changed, the resulting shift to the new equilibrium was considered as the emission-generating process. Whilst his model serves to emphasise that acoustic emissions are generated by relaxation processes, it is much too simplified for modelling the source functions of deformation or fracture processes in metals.

A more fundamental approach to modelling dislocation sources of acoustic emission has been attempted by Kiesewetter and Schiller [7] and by Mirabile [13], who apply the work of Eshelby [14] on dislocation motion. Eshelby treats the radiation from moving dislocations in an analogous manner to the electromagnetic radiation from an accelerating electric charge, and also calculates the acoustic energy radiated from an oscillating kink into the surrounding medium as a function of dislocation parameters [14]. Kiesewetter and Schiller [7] apply the result to the Frank-Read source, to obtain correlations with dislocation line length which agree with their experimental observations. However, it is not clear how justified they are in their simplifying assumptions about oscillation frequency in this particular application.

A recent approach which is already offering some success has been to model the acoustic emission source in an analogous manner to that used by seismologists for modelling earthquakes [15]. The simplest model [23] for an acoustic emission source is the point force monopole, whose time variation is a Heaviside function. The physical picture of such a source function is the final, rapid fracture of a tensile specimen, when the force on a very small area perpendicular to the force direction suddenly falls from some approximately constant value to zero. The important advantage of such a model is that it is possible to evaluate the surface displacements of the specimen due to the operation of the

source. The earliest formulation of the problem, for a surface source was by Lamb [16], but Pekeris [17, 18] solved the problem for a point source buried within the bulk of some material (the more usual case for acoustic emission during deformation).

It is possible to extend the analysis to sources having non-zero rise times and which may be represented by force dipoles, quadrupoles, or combinations of multipoles with variable orientations, in order to describe more realistically the force relaxations occurring in the vicinity of some dislocation motion or crack growth event. Nevertheless these point force models of the source are inadequate for a complete description of, for instance, a crack front of given length and prescribed shape, which starts to grow at constant velocity and then stops. In addition to the magnitudes of the force relaxations, and their time dependence, it is also important to take into account the extended nature of the source. The general case is extremely complex and has yet to be solved, but Burridge and Willis [19] and Willis [20] have obtained solutions for expanding self-similar cracks, whilst Simmons and Clough [21] have examined the effects due to coherence for extended sources. Work is in progress at a number of laboratories to apply this type of analysis specifically to acoustic emission sources, and the results are awaited with interest.

To date, little consideration has been given to modelling a dynamic source event, in particular when the source velocity approaches the shear wave velocity of the material. Roy [22] has extended the existing theory for a stationary point source to the case where it is moving at constant velocity along a line inclined to the surface. His results show that for subsonic velocities the generated elastic waves differ only in

amplitude from those of a stationary source. These effects could become important for rapidly growing cracks.

2.2 Elastic Wave Propagation

During the operation of a source, elastic waves are generated and it is important to understand their propagation behaviour within a solid. Pekeris and Lifson [23] have calculated both the vertical and horizontal components of the surface displacements at various positions on the surface of a half-space, for a monopole source with Heaviside function time dependence. Their analysis shows that the initial vertical displacement at the epicentre (the position on the surface vertically above the source, Fig 2) consists of a step function which has the same time dependence as the source, arrives at a time h/V_L (where h is the depth of the source and V_L the longitudinal wave speed) and has an amplitude, d, related to the source force magnitude F by;

$$d = k \frac{F}{\mu h} \qquad (1)$$

where μ is the shear modulus and k can be calculated from the material elastic constants. Following the longitudinal wave arrival, the surface continues to rise until the time h/V_S when the shear wave reduces the velocity of the surface eventually to zero, to give a permanent displacement. This important result shows that it is possible to relate the time variation of a surface displacement waveform (ie an acoustic emission signal) to the time dependence of the force relaxation of the source event. Breckenridge, Tschiegg and Greenspan [24] and later Scruby, and Wadley [40] have used the fracture of glass capillaries and pencil leads to simulate a monopole source with Heaviside time variation

and have obtained remarkably good agreement with theoretical prediction.

A second feature of Pekeris and Lifson's calculation is that the shape of the surface displacement waveform is very sensitive to the distance of the observation position from the epicentre, Fig 3. When this distance is large, the surface displacement waveform is dominated by surface waves and it is not clear, at present, if the measurement of these can give information about the source. Certainly seismologists can infer details about the mechanism of earthquakes from measurements at large epicentre distances.

Recently, two groups of workers have solved the problem of elastic wave propagation in an infinite plate [26, 27]. They calculated the displacements of the surfaces of an infinite plate in response to a point source either on the surface or within the plate. This development should now enable properties of the source to be determined in bounded plate-like bodies in addition to the infinite half-space, and may prove important for the practical application of acoustic emission.

Although the simple source used by Pekeris and Lifson accounts for the surface displacement waveforms from breaking glass capillaries, Fig 4, it does not fully account for the surface displacements of acoustic emission waveforms from fracture events in metals [25]; source models based on multipoles are required for this.

An additional effect arises through the necessity for using practical specimens. In semi-infinite specimens, the wavefront from a source reaches the surface at the epicentre in a form closely related to that generated by the source, Fig 5. In a bounded specimen, however, the initial wavefronts reaching a point on the surface may have undergone multiple reflections, interference and mode conversions, Fig 6, so that the surface displacement waveform bears little resemblance to

the waveform generated by the source. Furthermore, the later portions of the waveform will represent the response of the normal modes of the specimen to a transient pulse stimulation within the material and therefore provide more information about specimen geometry than the source function. There have been a number of approaches to the determination of source properties from measurements of acoustic emission waveforms in bounded media.

First, provided that the conditions of time invariance and linearity can be satisfied (and this is often not the case) the problem can be considered in terms of convolution. If $\underline{Z}(t)$ is the source function, $\underline{S}(t)$ the impulse response of the specimen and $\underline{Y}(t)$ the actual displacement at a point on the surface;

$$\underline{Y}(t) = \underline{Z}(t) * \underline{S}(t) \qquad (2)$$

where * stands for convolution. Taking the Fourier transform of equation (2), the source spectrum $z(\nu)$ is given by;

$$z(\nu) = \frac{\underline{Y}(\nu)}{\underline{S}(\nu)} \qquad (3)$$

and $\underline{Z}(t)$ can be obtained from this by taking the inverse Fourier transform. Thus, if the acoustic emission spectrum is divided by the transfer function of the system it should, in principle, be possible to evaluate $Z(t)$. This approach, ie deconvolution, has been developed by a number of workers [28, 29, 20], with limited success. One problem, to which little attention appears to have been paid, is the effect of 'noise' which can lead to large errors [31]. It is surprising therefore that authors make no comment on the validity of their results, and do not discuss the frequency-dependent errors which are introduced by de-

convolution. It also proves difficult, in practice, to measure the transfer function of the specimen.

A second approach is to compare values of $\underline{Y}(t)$ directly (without deconvolution) and seek empirical differences which can be related to changes in source mechanism. In practice, this has generally been performed in the frequency domain [32-35]. However, even in this approach uncontrollable variables can make it difficult to assess the validity of a result. Probably the most serious of these is that the transfer function, and hence the response of the normal modes of the specimen, is itself a function of the source position, $\underline{x}$, within the deformed material, so that equation (2) becomes

$$\underline{Y}(t,\underline{x}) = \underline{Z}(t) \cdot S(t,\underline{x}) \qquad (4)$$

Metals attenuate ultrasonic waves and it is necessary to consider the effects of material attenuation upon the propagation of acoustic emission waveforms. The degree of attenuation of an ultrasonic waveform depends upon both material properties (elastic constants, grain size) and wave properties, eg mode of propagation (L, S or surface wave) and frequency. Papadakis [36, 37] and Latiff [38] have tabulated attenuation coefficients for bulk waves in a range of materials and have discussed the changes in these coefficients as the frequency is varied. In the majority of experiments the measurable effect of material attenuation is reduction in amplitude of the high frequency components of the waveform. Thus, the source to detector distance should be minimised to reduce the effect, or the frequency dependence of the attenuation should be measured and taken into consideration.

2.3 The Detector

The surface displacement waveform produced by an acoustic emission source is detected with a transducer. The transducer converts mechanical vibrations of the specimen into electrical signals which can then be amplified and processed to provide information about the source.

Detection by a transducer of a surface displacement waveform causes the surface displacement $\underline{Y}(t,\underline{x})$ to be convolved with the transducer response function $T(t)$;

$$V(t,\underline{x}) = \underline{Y}(t,\underline{x}) * T(t) \qquad (5)$$

where $V(t,\underline{x})$ is the electrical output of the transducer. The ideal transducer should separately measure horizontal and vertical components of surface displacement (or velocity) at a point on the surface (since these are what we can calculate from theory) and linearly convert them into electrical signals over a bandwidth covering the full spectrum of the surface displacements. This bandwidth could extend up to, or even above, 100 MHz. For example if we consider the creation of a 30μm long crack in steel, growing at about 10% of the shear wave velocity, that is at 300 m/s, then the source lifetime would be about 10^{-7}s, and elastic waves with frequencies up to and above 10 MHz would be generated. Higher velocities and/or shorter cracks could generate much higher frequencies. In addition, the transducer must have sufficient sensitivity to detect the small displacements caused by the arrival of the acoustic emission pulses, which are usually $<10^{-10}$ m. Such a transducer does not, at present, exist. The majority of acoustic emission signals are detected with piezoelectric sensors (often constructed from lead zirconate titanate) which have a high sensitivity (detecting displacements$>10^{-14}$ m), but which only respond over a narrow

band about their resonance frequency, which is usually in the range 50 to 1000 kHz. All transducers impose limitations upon the amount of source information that can be retrieved from the detected signal and we shall now consider these.

Piezoelectric transducers with resonances below about 1 MHz, have sensitivities which drop rapidly at higher frequencies, even when damped. This makes it impossible to cover fully the spectrum of $\underline{y}(t,\underline{x})$ and hence the source spectrum. Therefore their use should be restricted to detecting and locating the positions of weak emission sources. Attempts have been made to use them in a standardised manner and to compare qualitatively the activity from different processes, by for example amplitude or energy distribution analysis. When this is carried out, great care has to be taken because only a fraction of the frequency spectrum is monitored and the distribution of energy within a source spectrum can vary between events so that the energy measured in a narrow frequency band is not a known constant fraction of the total. True, quantitative comparisons of energy are only feasible if the full frequency bandwidth of the source is covered by the detector.

It is important to note that even over its operating bandwidth the mode of operation of a piezoelectric transducer may change, with a part of its operating range being displacement sensitive and other parts being velocity or perhaps acceleration sensitive [39], depending on the position and width of its resonance. In principle, it does not matter which of the three quantities, displacement, velocity or acceleration, is actually measured in an acoustic emission experiment, provided it is known, because they are all inter-related by simple differentiation and integration operations. However, there are often

practical limitations which decide the form of detector to be used. For example, there is a lower frequency limit for accurate integration and similarly an upper frequency limit for differentiation. If meaningful comparisons between different experimentalists are to be made, it is necessary that transducers with a standard operation mode should be universally used.

Although it is possible to standardise measurements with piezoelectric transducers it is not possible to perform an absolute calibration on them at present, ie the voltage output of the transducer cannot be absolutely related to the surface motion. Capacitance transducers developed over the last five years at the National Bureau of Standards [24] and at Harwell [40] do not suffer from this drawback. They can be constructed to be displacement sensitive over a frequency range extending from dc to more than 50 MHz with a calibrated response. They are, however, less sensitive than a resonance device, able to detect displacements of $\geq 10^{-12}$ m. Because of this limitation, capacitance transducers are restricted to monitoring the more energetic acoustic sources. This can prove a serious limitation in some low strength materials, but less so during fracture in high strength or brittle steels.

2.4 Signal Processing and Interpretation

Bolin [41] has produced a bibliography listing recent papers dealing with both the signal processing and interpretation of acoustic emission signals whilst Stone and Dingwall [42] have critically discussed the significance of many of the commonly measured parameters of such signals. Consequently, these will only be briefly considered here. Before we do this, however, there are some general points which

should be borne in mind when attempting to measure acoustic emissions.

In any acoustic emission test it is important to maximise the signal-to-noise ratio, and if this is to be done without reducing bandwidth then that means reducing the background noise level whose chief origin is electromagnetic interference and amplifier white noise. Sometimes, spurious signals are recorded, eg from friction rubbing at the gripping points on a tensile specimen. This problem can be overcome by the careful choice of specimen test geometry and, if need be, by the use of several transducers not only to detect but also to locate the origin of each emission. Another major problem is the very wide dynamic range of acoustic emission signals, whose displacement amplitudes may be less that 10^{-15}m and sometimes more than 10^{-9}m, a range of 10^{6}. In addition, the rate of generation of acoustic emission signals can vary considerably. In some experiments, so-called 'continuous' emission has been observed where the low amplitude acoustic emissions are generated at such a high rate that they overlap in time to produce the effect of a high "white" noise level. On the other hand other experiments have generated perhaps only three or four detectable so-called "burst" emissions (high amplitude, discrete events) during a test lasting several hours.

These properties of acoustic emission mean that it is difficult to use a single, all encompassing parameter to describe an experimental result uniquely. The most common ways in which signals have been processed in the past are:

(i) Counting
(ii) Energy analysis
(iii) Amplitude analysis
(iv) Frequency analysis

2.4.1 Counting

Counting the number of times the signal amplitude exceeds a preset threshold during an experiment (the cumulative ringdown count) or its time derivative (the ringdown count rate) constitutes the commonest method of displaying an acoustic emission result [43]. A lesser used technique is to count the number of acoustic emission events. The number of ringdown counts for an event detected by a transducer is [44]

$$N = \frac{\nu_R}{\beta} \ln \left(\frac{v_o}{v_t}\right) \qquad (6)$$

where ν_R is the resonant frequency of the transducer

β the lorarithmic decrement

v_o the initial voltage

v_t the threshold voltage

The limitation of this technique is that the results are strongly influenced by the geometry of the specimen, the properties of the detector and its bonding to the specimen, the precise detection threshold and the performance of amplifiers and filters. These combine to introduce both a degree of irreproducibility in measurements and great difficulty in standardisation of method which is so important for systematic studies. It is also quite impossible to relate ringdown count measurements to properties of the source function and it is therefore hoped that the decline in the use of such techniques for fundamental studies will continue.

2.4.2 Energy Analysis

The acoustic emission energy is generally assumed to be proportional to the integral of the square of the transducer output voltage.

The energy is usually measured after amplification of 80 to 100 dB, and over a limited bandwidth of typically 1 MHz. The commonly measured root mean square (RMS) voltage is closely related to the energy rate (ie acoustic emission "power"). It is not possible to relate the measured energy to the acoustic wave energy for a variety of reasons (see for example Curtis [45]). Two of the most important of these are uncertainty in the mode of transducer operation and only partial coverage of the source bandwidth by the detector (discussed above).

If a velocity sensitive device is used (output voltage v proportional to surface velocity u), then the electrical energy E_e is proportional to the acoustic energy incident on the transducer, E_a ie

$$E_e \propto \int_{-\infty}^{\infty} v(t)^2 \, dt$$

$$\propto \int_{-\infty}^{\infty} u(t)^2 \, dt$$

$$\propto E_a \qquad (7)$$

In the frequency domain, using Rayleigh's theorem [46]

$$E_e \propto \int_{-\infty}^{\infty} [U(\nu)]^2 \, d\nu \qquad (8)$$

where $U(\nu)$ is the Fourier transform of $u(t)$.

However, for a displacement transducer (v proportional to surface displacement x) E_e is no longer proportional to E_a since

$$E_e \propto \int_{-\infty}^{\infty} [x(t)]^2 \, dt \qquad (9)$$

A relationship between the energies can be derived in the frequency domain because [46]

$$U(\nu) = 2\pi i \quad X(\nu) \tag{10}$$

Hence
$$E_e \propto \int_{-\infty}^{\infty} \frac{[U(\nu)]^2}{\nu^2} d\nu \tag{11}$$

Comparison with (8) shows that the energy spectrum now contains a frequency dependent term. This frequency dependence of the measured energy can be eliminated by differentiation of the voltage signal prior to squaring and integration.

The effect of bandwidth on measured energy is illustrated by considering a rectangular pulse of amplitude A duration τ, and system bandwidth $\Delta\tau$ about the frequency ν_o.

Then
$$E = 2A^2\tau^2 \left[\frac{\sin(\pi\nu_o\tau)}{\nu_o\tau}\right]^2 \Delta\tau$$

Thus no quantitative relationship can be drawn between electrical and acoustic emission energy unless the pulse duration and bandwidth are known.

The advantage of using RMS or energy measurement is that it gives a continuous measurement of a parameter of the emission which can be standardised and used for comparative experiments. It must be emphasised, however, that extreme precautions have to be taken if this is to be related to some source property.

2.4.3 Amplitude Analysis

In this technique, which Ono [47] has recently reviewed, the amplitudes of the voltage signals from a piezoelectric transducer are plotted as distributions and then compared. It has commonly been

found that the number of signals exceeding a specified level is given by:

$$N(a) = \left(\frac{v}{v_o}\right)^{-b} \qquad (13)$$

where v is the amplitude of a transducer voltage amplitude level

v_o is the lowest detectable amplitude

and b is the distribution characteristic.

The b value has been used to characterise emission from different processes. Typically b is in the range 0.2-0.4, small b values being indicative of a high proportion of energetic relaxation events. There is however no fundamental importance in the precise b value measured in an experiment, but it can serve empirically to characterise different forms of emission [48].

2.4.4 Frequency Analysis

Some of the implications and limitations of frequency analysis have already been discussed in previous sections and we have seen that frequency analysis could yield information about source rise time and fracture type. However unless extreme precautions are taken the analysis is limited to the observation of changes in the frequency spectrum which hopefully can be correlated with different types of deformation process. The most commonly employed method of extracting frequency information from emission is a digital one in which the emission waveform after amplification is passed into a transient recorder to digitise the waveform for subsequent access into a small computer. Standard Fourier transform routines then permit frequency analysis. This digital approach requires a digitisation frequency of at least twice that of the maximum expected frequency and

so even broad bandwidth systems are currently technology limited to about 50 MHz because the maximum digitisation rate is about 100 MHz. However almost all frequency analysis has been done with narrower bandwidth systems with an upper frequency limit of about 5 MHz. Digital techniques require a lot of instrumentation and much of the early work was done by direct observation or by photographic recording and visual analysis of shape change. Mullin and Mehan [49] applied frequency analysis to boron and carbon reinforced epoxy systems and by analysing the pulse shape changes of emissions photographed on an oscilloscope showed that different frequencies were associated with different failure processes in the composite. Unfortunately their work was not rigorous and it is difficult to know how much reliance to place on their results. Graham and Alers [50] applied frequency analysis (over a 2 MHz range) to emissions produced during deformation and fracture of a pressure vessel. They found two distinct types of spectra; one which was associated with plastic flow and the other with crack extension. Rather surprisingly, in view of the limited bandwidth and the bounded system, they found the results were independent of the type of test and sample geometry. Speake and Curtis [51] using a limited bandwidth detection system but using constant geometry specimens and varying only the fracture process, were able to show that changes in frequency content of the detected emissions could be correlated with different failure processes in carbon fibre reinforced plastics.

This significant result showed that different types of failure process could be identified by frequency analysis as long as other variables were controlled. This finding has also been supported by Ono and Ucisik [52] who analysed the emissions from compact tension specimens of three high strength aluminium alloys.

3. Acoustic Emission During Plastic Deformation

The mechanisms of deformation and fracture which generate detectable acoustic emission are only recently becoming understood. The aim of this chapter is to clarify our understanding of the source of emission in terms of dislocation dynamics, in the light of these recent studies.

The experiments reported up to about 1973 have been extensively reviewed by others, (53-56) and it was abundantly clear that the emission was generated by the motion of dislocations but that the mechanism of deformation could have a profound effect upon the observed form of the emission. Ying [53], in his review, attempted to relate the strain dependence of the acoustic emission count rate observed by Fisher and Lally [6] from copper single crystals oriented for single slip to simultaneous changes in total dislocation density, Figure 7. Although a fair correlation after stage I was found, it was clear that yield and Stage I deformation generated considerably more emission than the model predicted. Attempts have been made by others to relate parameters of acoustic emission activity [57] (eg acoustic emission count rate) to the mobile component of the dislocation density, both in 7075-T6 aluminium [58] and alkali halide crystals [3]. However, the assumption that all mobile dislocations contribute equally to the observed emission also appears to be a gross over simplification.

A number of studies proposed models of acoustic emission sources based upon specific deformation mechanisms, eg Frank-Read source operation [5,58] or the unpinning of dislocations [6,59]. For both mechanisms the source of emission is envisaged as the rapid collective motion of a large number of dislocations similar to the model proposed by Fisher and Lally[6].

Let us now proceed to build a more complete description of the sources of acoustic emission during deformation and in particular, account for the dependence of emission activity upon microstructure variables such as grain size and composition. Throughout we have to remember that the measured emission bears little resemblance to the elastic waves generated at the source and consequently much of the ensuing discussion is, necessarily qualitative.

3.1 Single Crystals

Single crystals are the best metallurgically defined materials, and a considerable understanding has been gained of their deformation mechanisms. The emission from face centred cubic single crystals is usually of the so called continuous type and consequently individual events cannot be observed. The inference of the source mechanism rests on a comparison of the strain and strain rate dependence of the emission and deformation behaviour.

Jax et al [61, 62] have observed the emission count rate and RMS voltage from single slip oriented crystals of copper, both as a function of strain and strain rate. During constant strain rate deformation they observed a sudden rise in emission count rate during Stage I, followed by a steady decrease as the workhardening rate increased, Figure 8. The emission rate at a particular strain also increased with increasing strain rate, presumably only because the rate of source activation had also increased, rather than the initiation of a new strain rate sensitive emission source. Jax et al postulated the emission source to be the unpinning of dislocations resulting in the propagation of groups of dislocations across a slip plane. The strain dependence of the emission was attributed to a strain dependence of the mean free path of unpinned dislocations which is a maximum at the start of deformation and decreases

during Stage II deformation.

Kiesewetter and Schiller [7] reported a similar strain and strain rate dependence for the emission from aluminium single crystals, Fig 9. Unfortunately, the difference in apparent emission behaviour between aluminium and copper crystals of similar orientation cannot be directly attributed to changes in deformation behaviour because of the absence of a standardised measurement technique. Kiesewetter and Schiller observed, like Jax, that the mean square emission voltage was proportional to strain rate $\dot{\varepsilon}$. Since the strain rate is given by

$$\dot{\varepsilon} = \lambda_m b \bar{v} \qquad (14)$$

where λ_m is the mobile dislocation line length, b is the Burgers vector and $\bar{v}$ the mean dislocation velocity (a constant for changes of strain rate since the flow stress did not vary significantly), they considered the emission increase with strain rate to be due to an increase in moving dislocation line length. This postulate was also consistent with the observation that the mean square emission was proportional to crystal length at a particular flow stress and strain rate.

Using Eshelby's theory [14] of the elastic radiation from an oscillating screw dislocation, they proposed that the emission dependence upon strain resulted from a reduction in the size to which dislocation loops (generated from Frank-Read sources) could expand. Unfortunately, their support for this model was based upon the assumption that the mean dislocation velocity did not vary during deformation from yield to fracture. This is an over-simplification; it is well known that dislocation velocity is proportional to flow stress in aluminium and it is quite possible for

the mean speed of dislocations to vary by as much as a factor of 100 during a test.

A weak aspect of all these theories of acoustic emission sources has been the lack of information about dislocation motion occurring during an experiment. Imanaka et al [63] extended normal measurements of acoustic emission and stress strain behaviour. In a novel experiment they simultaneously monitored the stress, strain, acoustic emission amplitude and count rate, and the ultrasonic attenuation of 27 MHz longitudinal waves during compressive deformation of copper single crystals.

They deduced that the deformation sequence during this experiment was initiated by dislocations detaching themselves from impurity atom pinning points at low stress levels. As the stress rose, the free dislocation segment length increased toward a critical value of 10^{-6}m. Once the critical length was reached rapid dislocation multiplication occurred by the activation of Frank Read sources. They suggested that the emission source during this sequence of events was the sudden (timescale less than 4×10^{-6}s) increase in the mobile dislocation density associated with Frank Read source operation.

The origin of the emission in both copper and aluminium appears the same; namely the sudden release of dislocations from a source followed by their propagation as a group over an appreciable fraction of the crystal glide plane. Emission may, as mentioned in 2.1.2 be the Eshelby radiation accompanying dislocation accelerations, or it may be just the re-arrangement of the elastic strain energy field following an abrupt local plastic relaxation. However it is clear that not every motion of each dislocation is detected in a test. Those events incorporating the greatest number of dislocations moving over the largest fraction of the glide plane will be

most easily detected. Less energetic motions could generate signals below the limit of detection and would consequently fail to contribute to the emission signal from the transducer. Processes which restrict the magnitude of slip events, for instance the forest interaction, cause a reduction in acoustic emission activity, and are the origin of the loss of emission after deformation to high strains.

The strain dependence of acoustic emission activity would, we expect, be dependent upon crystal orientation, stacking fault energy, composition and test temperature, since each influences the magnitude of slip events.

The effect of crystal orientation upon the strain dependence of the emission voltage has been reported by Kuribayashi et al [64]. They observed the acoustic emission from 99.9% aluminium crystals with four orientations; in all cases, the emission-strain relation was similar to that observed by Kiesewetter and Schiller[7]. However, the degree of emission at a fixed strain was dependent upon crystal orientation. The greatest activity was observed at strains of 0.5 to 0.7% from crystals with orientations either close to the middle of the <001>-<111> boundary or at the centre of the <100><110><111> stereographic triangle. The least activity was observed from the crystal with an orientation about halfway along the <100>-<110> boundary. However, these differences became less apparent after deformation to high strains. Although there have been detailed studies of the orientation dependence of slip processes [65] the results of Kuribayashi et al are apparently not simply interpreted. In particular, the observation of similar levels of emission from crystals with single and multiple slip orientations would not have been expected and remains unexplained.

Changes of stacking fault energy are expected to have a significant

effect upon the emission activity because it is this parameter which determines the ease of cross-slip, and the degree of strain localisation within a slip band. Hatano [66] has used wideband recording techniques (0.1 to 4 MHz) to monitor the acoustic emission power accompanying the deformation of a range of materials with different stacking fault energies. The peak acoustic emission power recorded during systematic testing of the materials is shown in Table 1, and it is clear that the emission decreases rapidly with decreasing stacking fault energy. This is consistent with the emission increasing with ease of cross-slip. However, the results need to be treated with caution because other metallurgical variables, which can also modify the acoustic emission, were uncontrolled in these experiments. Somewhat surprisingly, acoustic emission was most energetic when deformation was lease localised by high stacking fault energy. Siegel [67] in a related study with polycrystals, reported a strong dependence of emission activity upon

TABLE 1

Acoustic Emission Power and Stacking Fault Energy for some FCC Metals

Material	Stacking Fault Energy/$\mu J\ cm^{-2}$	Acoustic Emission Power/pW	
		(a) Single Crystals	(b) Poly Crystals
Cu	410	4	1.3
Cu-0.34% Al	390	1.2	-
Cu-1.15% Al	330	0.08	-
αBrass (70 Cu-30 Zn)	140	-	0.06
Stainless Steel (18 Cr-8 Ni)	100	-	0.00

stacking fault energy during unloading. He related the increased emission from low stacking fault energy metals to the larger reverse plastic strains.

A number of important experiments have not been performed to date. Temperature variations, despite their well known effects upon dislocation motion, have not been studied, presumably because of simultaneous variations in transducer/couplant efficiency. In addition there is a need for a series of systematic experiments to study the influence of crystal structure, composition and microstructure.

3.2 FCC Polycrystals

One way of testing the models used to account for the emission from single crystals is to study the emission activity, when one component of the microstructure (which affects the source process) is systematically varied, eg the grain size. One effect of reducing the grain size is to restrict the area of individual slip events which should therefore lead to a reduction in emission activity.

Bill [68] has reported the effect of grain size upon the acoustic emission count for both aluminium and copper. For aluminium, little emission was observed for strains $\leq 5 \times 10^{-4}$ and no grain size dependence was found. However, when the metal was strained to 2% a strong grain size dependence was measured (Fig 10) which was much greater than the corresponding yield stress dependence. Bill suggested that the emission was generated by the operation of 'unstable' dislocation sources located near grain boundaries. Such sources were considered to be activated during the progression of slip from grain to grain. The grain size independence of the emission activity during microstrain was attributed to an emission source controlled by the forest dislocation distribution (grain size independent).

The results obtained by Bill and their interpretation demonstrate the severe problems encountered in the interpretation of continuous emission measured by a counting technique. Kiesewetter and Schiller [7] have measured the mean square voltage when the grain size of aluminium was varied in the range 0.05-2 mm. The emission from each specimen showed a similar flow stress dependence, but in contrast to Bill's work, the emission activity increased with increasing grain size approaching that of a single crystal, Fig 11. These results were interpreted by considering the systematic changes in slip increment accompanying changes of grain size. For single crystals, typical slip increments were in the range 5-20μm, the lowest values being observed after extensive work hardening, the highest values being found at yield. The displacement of the characteristic curve of polycrystals below that of the single crystal was then considered to reflect the reduction in slip area when grains with several intersecting slip systems are deformed.

Kishi et al [69] also measured the RMS emission using a resonant transducer during the deformation of polycrystalline aluminium. They tested four specimens of 99.9% purity aluminium with grain sizes of 30, 43, 60 and 94 μm. The emission activity of the two specimens with largest grain size was similar, but reduction of grain size led to an increase in emission activity. According to the simple model discussed above, the emission activity should decrease with decreasing grain size. The discrepancy between model prediction and experimental observation could be a consequence of the higher impurity concentration in Kishi's material. This could serve to restrict co-operative dislocation slip processes to specimens with the highest flow stresses (smallest grain size) due to the drag of the Cottrell atmospheres. Further work is required to resolve this

inconsistency.

The errors that can be introduced through equipment limitations and which are rarely discussed in the literature, have recently been highlighted by a systematic study of the grain size and frequency content dependence of the acoustic emission from 99.99% purity aluminium reported by Fleischmann et al [70]. They measured the acoustic emission energy from deforming polycrystalline aluminium at three frequencies (0.94, 1.56 and 2.17 MHz). They observed, at each frequency, a similar dependence of acoustic emission activity upon strain to that reported by Kiesewetter and Schiller [7] with a maximum just after yield. However, at constant grain size, the position of the emission maximum was shifted to higher strains and the breadth of the peak widened as the observation frequency increased. In addition, when the grain size was varied, the position of the peak at fixed frequency moved to higher strains with increasing grain size. These results were interpreted by recourse to a model in which the lifetime of each slip event that generated an acoustic emission signal was proportional to the obstacle spacing (sessile dislocations or grain boundaries). As the obstacle spacing decreased the lifetime of each emission event was reduced and led to an increase in the higher frequency components of the emission. Thus, restriction of the frequency window through which measurements are made can lead to considerable errors which casts a degree of doubt on the validity of all narrow band results.

The origin of acoustic emission from single crystals appears with only small modification to account for some of the measurements made on fine polycrystals. Major ambiguities remain however, and it is important that the true grain size dependence for fcc metals be measured accurately to confirm the results of either Bill [68] or Kieswetter and Schiller [7].

3.3 Non-Ferrous Alloys

Another microstructural parameter that will modify the sources of emission is material purity since it can affect both the magnitude and time dependence of slip events.

The most frequently reported experiments have been performed with aluminium alloys and, to a lesser extent, brass. In most tests two components of acoustic emission (burst and continuous) are observed, but the proportion of each and the total of both, is often very dependent upon the detailed composition and heat treatment of the test material [57, 66].

A great diversity in acoustic emission activity has been observed during the deformation of aluminium alloys. During constant strain rate experiments most acoustic activity is usually (but not always) observed in the vicinity of yield [4, 60, 62, 70-72]. Two types of model have been used in an attempt to explain the source process.

3.3.1 Dislocation Models

Agarwal et al [59] have reported the acoustic emission activity associated with the deformation of solution treated and room temperature aged 2024 aluminium alloys. They observed a rapid decrease in acoustic emission count as the ageing time was increased, the count only returning when the material had been overaged at higher temperatures. Jax et al [61] have reported some of the work of Zeittler who observed similar trends in yield emission activity during the deformation of isothermally aged $AlCuMg_2$ alloys, Fig 12. Wadley and Scruby [2] and Fenici et al [74] have independently made studies of the effect of ageing on the acoustic emission from high purity Al 4wt% Cu and obtained similar results. In the former study solution treated material was systematically aged at 170°C for periods up to 48 hours. There was a pronounced increase in yield emission activity

after the quenched material had been aged for short periods of time. However, the detected emission energy depended critically on ageing time, and increased to a maximum after about 2 hours before decreasing again (Fig 13). This peak in activity, which occurred a long time before peak hardness (2-4 days at 170^{o}C), was observed when the microstructure contained a fine dispersion of Guinier-Preston (G.P.) zones, Fig 14. A simple model was proposed to account for the ageing peak, based on the changes in deformation mechanism as ageing progressed. In the quenched condition, deformation was homogeneous and continuous in as much as there were comparatively few obstacles (other than solute atoms) that could temporarily inhibit the motion of dislocations. As ageing progressed the obstacle (G.P.(I zones) strength increased and so the numbers of dislocations that could be held in a pile-up increased. As the stress then rose in the vicinity of yield it was conjectured that the dislocations could break through some of the obstacles leading to local precipitate reversion and a sudden strain increment thus generating acoustic emission. Continued ageing led to an increase in the strength of the obstacles and an inability in the yield region for dislocations to break through and reversion to occur.

Agarwal et al [59] also attributed the emission source during yield to the operation of dislocation sources, by estimating both the minimum dislocation length that could act as a dislocation source and the slip distance that produced a detectable displacement at the transducer. During ageing the average interparticle spacing decreased until at peak hardness it was about 0.05 μ m. Taking this value also to be the free dislocation length, the strains in peak hardened material were shown to be below the sensitivity limit of the detection system. This model adequately explains their observed decrease in activity during room temperature

ageing, and also the increase in activity in the overaged condition because of an increase in interparticle spacing to 2-3 μm. The two models are complementary, that of Wadley and Scruby [2] being applicable to early stages in ageing and that of Agarwal et al [59] being applicable to later stages.

Other workers, including Jax et al [61], Hatano [66] and Hamstad et al [72] have reported similar ageing effects in Al-Cu-Mg alloys, 2024 and 7075 aluminium alloys, together with the appearance of a second peak in emission in the plastic region. This second peak which can be seen in Fig 12 has not as yet been explained; it might be due to an interaction between dislocations and solute atoms (ie dynamic strain ageing) but further work is required before any firm conclusions are drawn.

3.3.2 Inclusion/Precipitate Fracture Model

Copious burst emission, observed in the yield region of some aluminium alloys, has been attributed to the fracture of inclusions and large precipitates that are always found in commercial purity aluminium alloys [75-77]. Although the fracture of brittle inclusions cannot account for many of the effects of ageing on acoustic emission activity, it is possible, under certain circumstances, for it to be a significant component of the total emission from a commercial grade aluminium alloy. Bianchetti et al [75] have observed a burst component of emission from 7075 T6, only when the batch of material contained large (20-60 μm) inclusions which underwent fracture during testing, Fig 15. The fracture of these inclusions, which were rich in chromium and contained traces of iron, magnesium, titanium and copper, was considered to be the source of many high amplitude burst emissions. Brittle inclusion fracture has also been considered to be a source of emission in 7075 T651 aluminium alloys [72]. Wadley and Scruby [77] have examined the emission from commercial purity Al 4 wt.% Cu and

Al 4.5 wt.% Mg alloys and observed many cracked inclusions after the fracture of specimens that exhibited burst activity in the yield region. However, further unpublished work to relate the rate of particle fracture to the strain dependence of the acoustic emission power has still not completely established that cracking is the dominant source of acoustic emission; most emission occurred in the vicinity of yield, but many inclusions fractured during the quiet period when the specimen had started to neck down.

The fracture of brittle inclusions in aluminium alloys has been extensively examined by van Stone et al [78]. Using stop tests they examined the strain dependence of inclusion fracture in 2014, 2024, 2124, 7075 and 7079 aluminium alloys and found that the fracture of cracked inclusions was proportional to strain, the constant of proportionality varying from alloy to alloy. In addition, they found that their data fitted the relation

$$\sigma_f = \frac{1}{q} \frac{6E\gamma}{d}^{\frac{1}{2}} \qquad (14)$$

where σ_f is the stress at which a particle of diameter d, Young's modulus E and surface energy γ, fractures. The stress concentration factor at the particle was q. Thus, the largest inclusions should fracture first during a tensile test, to generate large amplitude acoustic emission transients. The fracture of inclusions seems likely to be a source of acoustic emission in commercial alloys, but further confirmatory work is needed.

Two aspects of the emission behaviour of non-ferrous alloys have recently been reported but, as yet, received little systematic study. The first is the observation of the second acoustic emission peak associated with the plastic region in some alloys [60, 71]. The second is the

emission associated with dynamic strain ageing (Portevin-LeChatelier effect) [4, 61, 70, 76, 78]. Pascual [4] has observed an increase in emission prior to the occurrence of a type A serration load drop during serrated yielding, and an increase in emission during the occurrence of a type B serration load drop. He proposed that the emission source is associated with increases in the mobile dislocation density. Hatano [80] has observed the details of the emission during serrated yielding to change as the strain rate changes but has not attempted to relate this to dislocation behaviour. The sudden release of dislocations during the deformation of materials exhibiting the Portevin-LeChatelier effect, and the strain increment this causes, would seem ideal sources of acoustic emission, and it would be enlightening to ascertain the effects of grain size or of changing solute upon the emission.

3.4 Iron Base Alloys

A full understanding of the emission from ferritic steels should start with a detailed study of the emission from pure iron. There has, in fact, been very little work reported on the sources of acoustic emission in pure body centred cubic metals including iron. The closest approach has been a study by Higgens and Carpenter [81] who examined the sources of acoustic emission in pure iron containing between 0.005 and 0.017% carbon. They observed emission in both the elastic and plastic portions of the stress-strain curves. The former they attributed to stress induced motion of magnetic domain walls, and the latter to the breakaway of dislocations. One metallurgical variable, the grain size, which would be expected to affect such a process significantly, was not studied. However, Tandon and Tangri [82] have recently investigated the sources of acoustic emission during the tensile deformation of Fe 3% Si with variable grain size. Using

conventional counting techniques combined with extensive etch pit studies of specimens tested to different strains, they attempted to relate the emission-strain relation, Fig 16, to the strain variation of grain boundary dislocation sources and also examined the effect of grain size upon such processes.

During the microyield region about 100 bursts of emission were observed. Etch pit studies revealed the presence of dislocation pile-ups within grains close to the surface of the specimen; these pile-ups appeared to have been generated by grain boundary sources. They considered the origin of emission to be the co-operative activation of perhaps 300 such sources to generate a single emission pulse. As the specimen was further deformed a yield drop was observed. This was associated with the formation of a Luders band and an accompanying high emission rate, which was attributed to the operation of dislocation sources. The band propagated along the length of the specimen at approximately constant velocity and gave less emission activity than the yield did. This, they attributed to the localisation of deformation in a band about 25 grains across. Once the band had propagated the length of the specimen the operation of grain boundary sources was inhibited so that the emission rate dropped during work hardening.

The effect of grain size upon the emission count during microyield is shown in Fig 17 and during the interval between 90% of yield stress and 2.5% strain in Fig 18. The emission increased with increasing grain size during microyield but like Bill's observation with aluminium [68] decreased with increasing grain size during post yield deformation.

There have been a number of recent studies of the emission from ferritic steels. Three deformation processes have been proposed to account

for the majority of the observations:-

3.4.1 Luders Band Propagation

Copious yield region emission from mild steels has been associated with the initiation and propagation of Luders bands [33, 60, 82]. Again, most activity is observed during initiation of the band. Little systematic work has been reported, and one can only speculate that the emission source is similar to that proposed by Tandon and Tangri for Fe 3% Si. Acoustic emission accompanying Luders band motion has also been reported during serrated yielding of mild steel in the temperature range 200° - 300°C. [60, 82]. The origin of the emission is probably due to the sudden strain relaxations accompanying the escape of dislocations from solute pinning points.

3.4.2 Carbide Fracture

Several investigations have proposed the fracture of carbide platelets as the source of acoustic emission from pressure vessel steels [60, 83, 84]. This emission source is still in some doubt, since Ono et al [35] have been unable to identify carbide fracture categorically as the emission source in 4130 ferritic-pearlitic steel whilst Bentley and Birchon [83] considered the cracking of carbides to be definitely undetectable. At the present time, insufficient work has been reported to examine the influence of carbide composition shape and distribution upon the generation of acoustic emission. But it would be expected that platlet forms of austenite (eg in pearlite) are more likely to generate emission than the small spheroidised carbides present in quenched and lightly tempered steels.

3.4.3 Decohesion/Fracture of Inclusions

The brittle fracture of MnS inclusions has been postulated as a source of acoustic emission in commercial steels [35, 82]. The emission

activity has been found to depend upon sulphur content and the orientation of specimen with respect to the rolling axis. The results suggest that decohesion of the inclusion-matrix interface may well be the major emission generating process.

4. Acoustic Emission during Crack Growth

The sources of acoustic emission during the deformation of a uniaxial tensile specimen discussed in the previous section, can be considerably modified in the multi-axial stress state that exists in the vicinity of a crack, and may even be exhausted during the final stages of fracture. The addition of several modes of fracture, and their subtle dependence on detailed composition, heat treatment and testing conditions all lead to a great diversity in acoustic emission activity. Clearly a study of the emission characteristics (count rate, cumulative count, power, amplitude distribution etc) during the early part of a tensile test would, alone, be unable to predict the details of the mechanism of fracture. In this section we shall try to ascertain the processes of deformation and fracture that are sources of detectable acoustic emission in a crack propagation experiment, in particular concentrating on the problem of the quiet ductile crack [85, 86], environmentally assisted and fatigue fracture.

4.1 Ductile Crack Propagation

One might expect copious acoustic emission activity during crack growth because of the many large strain energy relaxation events involved. However, the many studies of acoustic emission during ductile crack growth (eg ref 85-101), reveal a wide range of activity: some materials emit large amounts of emission, but others are almost completely quiet. Ingham et al [85] have made a comparative study of the relative acoustic emission activity during crack propagation in a range of steels with yield strengths

between 230 and 1620 MPa, Table 2. The relative activity increased with increasing yield stress and decreasing ductility. Steels undergoing ductile fracture can (with only a few exceptions [87, 88] be broadly classified into one of two categories [85, 89-100]. In the lower strength, but tough, steels the majority of the emission occurs during the period of plastic zone expansion, and the increments of crack advance appear quiet [89-91], Fig 19. However, when high strength steels are tested, much of the activity occurs during the last 20% of the test and the processes associated with plastic zone expansion no longer dominate the total emission [92-100], Fig 20. This lack of emission during crack growth in low strength ductile materials has been termed the quiet ductile crack problem and has been a major drawback to the widespread application of acoustic emission to engineering problems (Section 5).

Table 2

The Relative Acoustic Emission Activities of Nine Commercial Steels during Crack Porpagation at Room Temperature

DECREASING ACTIVITY ↓

Designation	Type	Yield Stress MPa	Ultimate Tensile Stress MPa
300M	High strength steel	1615•	1960
BS 1501-261	Mo-B steel	405	623
BS 1501-271	Mn-Cr-Mo-V steel	515	638
BS 1501-151	Semi-Killed C-Mn Steel	232	431
BS 1501-213	Semi-Killed, Nb treated C-Mn steel	410	572
BS 1501-224	Fully-Killed Al grain-refined C-Mn steel	284	466
X60	C-Mn pipeline steel	405•	626
BS 1501-821	Austenitic stainless steel	342•	620
BS 1501-622	2¼ Cr-1 Mo steel	363•	543

• 0.2% Proof Stress

4.1.1 Plastic Zone Expansion

The acoustic emission during plastic zone expansion in a precracked specimen has been linked with the fracture of brittle inclusions and/or their decohesion from the matrix, carbide cracking and rather poorly defined dislocation processes. None of the proposed sources have as yet been conclusively shown to generate the major component of the emission during zone expansion.

The rate of acoustic emission activity from a typical low strength precracked steel specimen usually increases, and then decreases as it is loaded, and attempts have been made to relate the cumulative count to the plastic zone volume [89], ignoring the source process. Such relationships are highly speculative in view of the uncertainty of the emission source and the crude methods employed for monitoring the emission. Consider the series of events associated with the loading of a precracked steel specimen: as the specimen is loaded a stress concentration develops at the tip of the crack and when the source activation stress (or strain) for one of the processes described above is reached acoustic emissions are generated. The rate of generation of these emissions is then determined by the volume rate at which the activation stress propagates through the specimen. This model then needs further modification because experiments performed using tensile specimens [103] have clearly shown that emission sources operate over a range of stresses (or strains) and the assumption of a single activation stress is too simple. The emission rate is dependent both on the plastic zone volume increase rate and the stress dependence of source activation.

4.1.2 Incremental Crack Growth

Many of the high strength steels, and in particular, those with a low work hardening capacity, generate appreciable emission during crack

growth [92-100]. The emission has often been observed as high amplitude "bursts" generated during load drops in a constant extension rate test (the period when crack advance occurs) [94, 96-98, 100]. Attempts have been made to relate areas of crack advance to some parameter of the emission [93, 96, 97]. Desai and Gerberich [96] have for instance proposed a relation between acoustic emission amplitude, A, and crack increment area, Δ, of the form;

$$A = \frac{2.5\, m\, k\, W^{\frac{1}{2}}}{YLB}\, \Delta \qquad (15)$$

where k is the applied stress intensity, L is the distance between the grips, W the specimen width, B the specimen thickness, Y is a function of (a/W), a is the crack length, and m is the proportionality constant between stress wave amplitude and the load drop per unit thickness.

Work by Scruby et al [25, 102] also shows a linear relation between emission amplitude and crack increment area, but only when the surface displacement of the direct longitudinal wave is measured at the epicentre. In their broadband study the specimen was designed to minimise distortion of these elastic waves after they are released by a crack propagation event. The source was restricted in position so that it was vertically beneath a transducer, at a depth h. A calibrated capacitance transducer was then used to record the vertical displacement of the specimen surface and this was compared with theoretical predictions based upon work by Willis [20] and Pekeris [23] (Section 2.2). They proposed that for a monopole source the amplitude of the leading edge of an acoustic emission signal, d, could, using equation 1, as a first approximation be related to the incremental crack area Δ by the relation:

$$d = \frac{0.047\, \sigma_\ell\, \Delta}{\mu\, h} \qquad (16)$$

where μ was the shear modulus, and $\sigma\ell$ the stress in the vicinity of the crack event. The result is not applicable to most conventional experiments because d is never measured with a displacement sensitive calibrated transducer, h is usually an unspecified variable and the transducer is often not situated at the epicentre.

Despite these reservations concerning quantification of data, it is clear that in some materials crack growth generates copious bursts of emission. A problem that is yet to be solved is why some materials generate detectable acoustic emission during ductile crack propagation whilst others do not.

An important factor is the yield stress of the material. It is clear from equation 16 that if the mechanism of emission were unchanged the amplitude of the emission would be proportional to the local stress, and since acoustic emission detection systems have a sensitivity threshold, it is conceivable that some elastic waves released during crack growth in low yield strength materials might go undetected. Another possibility is that the fracture mechanisms in high strength materials are different from those in low strength materials. Thus, the incidence of quasi-cleavage has been proposed as a possible emission source in some materials [85, 94] whilst "pop-in"appears to generate discrete emissions in maraging steels [99].

Clark and Knott [100] have proposed a mechanism of emission for materials with a low work hardening capacity ($\sigma_y : \sigma_{UTS} \sim 0.8$) that may account for the high activity in some low alloy (and possibly maraging) steels. They have examined the emission during crack growth in three steels and observe most emission in material with least work hardening capacity and have attributed the emission to the onset of fast shear of

inter-inclusion ligaments. Such a fracture mode has been observed as a zig-zag fracture topography [102], the individual shear facets being up to 1 mm in length [103]. The fast shear of an inter-inclusion ligament (which can be likened to the fracture of a small tensile specimen) at the head of a crack would, because of the attendant sudden strain relaxation, be expected to be an energetic emission source. It is, however, not clear at present which of the detailed processes taking place during such a fracture is the source of the detectable emission. One possibility is the intense shear deformation when local strains ≥ 1 can be produced, but emission could also be associated with the microvoid linkage mechanism when final separation occurs, or some complex combination of both.

Nevertheless, it does appear that this fast shear mechanism acts as a dominant source during ductile fracture, whereas the classical void coalescence process appears to generate little detectable emission. These findings are consistent with both the broad [102] and narrow band [104] results of Wadley and Scruby using a quenched and systematically tempered low alloy steel, although here the emission source during local shear appeared to extend over areas of several hundred square micrometres rather than the area of the shear wall (up to several square millimetres).

4.2 Environmental Fracture

Acoustic emission has from an early stage in its development appeared a useful technique for detecting the onset of cracking during hydrogen embrittlement or stress corrosion cracking, firstly, because both phenomena often induce a brittle mode of fracture in an otherwise ductile material, and secondly, because high strength steels are particularly prone to such phenomena. Duneçan and Tetelman [105] have used acoustic emission to monitor the onset of cracking in hydrogen charged

AISI 4340 steel and proposed a relation between count rate, dN/dt, and stress intensity factor, K of the form:

$$\frac{dN}{dt} = 6.7 \times 10^{-5} K^5 \qquad (17)$$

Such a specific relationship between the emission count rate and the stress intensity is somewhat controversial and, bearing in mind the crudeness of the emission monitoring technique used, must be regarded as a purely empirical finding with very restricted applicability.

It is clear from experimental studies, eg Chaskelis, Cullen and Krafft [106], that the emission rate during hydrogen embrittlement did increase with increasing stress intensity during aqueous stress corrosion cracking of 4340 steel. However, the emission rate was also sensitive to the microstructure of the steel. When other conditions were kept constant the emission decreased as the tempering temperature of the steel increased, (perhaps as a consequence of the restoration of work hardening capacity, or the reduction in yield stress).

The use of acoustic emission techniques during environmentally assisted fracture is proving to be a useful, empirical indicator of the initiation of cracking [106, 107], but as yet has made little contribution to our understanding of the micromechanisms of fracture. Wadley and Scruby [102] in an exploratory study have applied broad band techniques to the fracture of hydrogen precharged low alloy steel that had controlled microstructures, in an attempt to examine the relationships between emission rise-time and amplitude and the mechanism of fracture. During hydrogen assisted inter-granular fracture a range of risetimes was observed which was consistent with fracture by a series of jumps covering areas from one to five grain boundary facets. However, much work still

needs to be done to further quantify the data.

McIntyre and Green [109] have studied the acoustic emission activity of three steels, 817M40, 897M39 and AIS14340 during stress corrosion cracking in 3.5% NaCl solution and during gaseous hydrogen embrittlement. The acoustic emission activity in each steel was related to the area of crack advance, but they found that the average acoustic emission energy (measured over a 26 dB dynamic range) per unit crack extension (dE/dA) was dependent not only upon steel composition and microstructure but also crack environment, Table 3.

Table 3

The Effect of Metallurgical and Environmental Variables upon the Acoustic Emission Energy per Unit area of Crack Advance during Fracture of Three Steels

Steel	Grain Size/μm	Fracture Path	Environment	$\frac{dE}{dA}$ $(10^{-2} V^2 s\ mm^{-2})$
817 M40	17	Intergranular	3.5% NaCl	9
"	100	"	"	108
"	17	"	H_2 at 200 torr	31
897 M39	10	Transgranular	3.5% NaCl	5
"	10	"	H_2 at 190 torr	2
"	10	"	H_2 at 760 torr	1.5
AISI 4340	11	Intergranular	3.5% NaCl	31
"	200	"	"	210
"	11	"	H_2 at 200 torr	37

The intergranular mechanisms of fracture generated more acoustic emission in the dynamic range over which measurements were made than the transgranular mechanisms, suggesting that individual emission generating

events during intergranular fracture cover, on average, larger areas compared with transgranular fracture. Increasing the grain size during intergranular fracture also led to a proportional increase in emission area, again as a possible consequence of increased crack increment area. Finally, tests performed in hydrogen gas (as opposed to NaCl solution) led to larger emission events, possibly because of the higher availability of atomic hydrogen.

4.3 Fatigue Crack Growth

Acoustic emission techniques can be extremely sensitive indicators of the onset of cracking, and have been applied to fatigue cracking studies by a number of workers [109-113]. The high sensitivity can lead to problems in interpreting the emission and unless great care is taken the data may have little direct relation to the growth of fatigue cracks [113]. Thus, there have been reports of spurious emissions due to both frictional effects at the grips and machine noise [110]. Perhaps more importantly, acoustic emission signals have commonly been observed during crack closure and have been attributed to crack face rubbing [110], and this source of emission could mask that due to incremental crack growth unless care is taken to ignore emissions during crack closure [113].

If suitable precautions are taken it would appear that the technique can give qualitative additional information about the initiation of crack growth in favourable materials [112]. The extension of the technique to the measurement of crack advance has, to date, met with limited success [110], and requires systematic work to relate emission parameters to crack advance. Despite a number of detailed studies, the technique has not provided a great deal of additional insight into the mechanisms of fatigue crack propagation.

5. Applications of Acoustic Emission

No attempt is made here to review the wide range of technological applications to which acoustic emission monitoring has been applied (for reviews of these see references 1, 56, 114-123). We shall briefly aim to discuss the consequences of our earlier findings for current techniques as reliable monitors of structural integrity. In general, technological applications have concentrated upon three problems:

1. Detecting the presence of flaws.
2. Locating the position of flaws.
3. Assessing the significance of flaws.

In common with other non-destructive testing techniques the first and second problems have been tackled with some success, whereas the third is turning out to be extremely complex.

5.1 Detecting the Presence of Flaws

It was shown earlier that a range of deformation and fracture processes in metals emit acoustic emission signals in laboratory experiments, and if these could be detected in an engineering structure, either during its fabrication, pre-service proof testing or in-service use, they would provide a valuable warning of impending failure. However, the background noise environment, against which the emission signals must be detected, can be so high that only the more energetic are detectable (1, 124, 125). Thus, materials which fail by brittle modes (eg cleavage, hydrogen embrittlement, stress corrosion cracking or temper embrittlement) may well generate detectable acoustic, and the sensitivity in terms of minimum detectable crack area could be much better than any other existing N.D.T technique. However, great care is taken nowadays to avoid failure by these processes, and the majority of engineering steels and aluminium

alloys are used in a tough condition where the normal failure mode would be by the slow ductile growth of pre-existing or creep-fatigue induced flaws. Laboratory experiments have shown that such crack growth processes can, in some circumstances, generate very high amplitude acoustic emission signals (eg high strength materials with low work hardening capacity), but often, and especially when crack growth occurs by slow void coalescence, little or no detectable emission has been detected. Thus, while crack growth in some pressure vessels constructed from maraging steels [126] has been reliably detected by acoustic emission techniques, pressure vessels constructed from lower strength C-Mn mild steels have failed with no release of detectable emission during crack growth [86]. The phenomenon of the quiet ductile crack throws considerable doubt upon the viability of acoustic emission as a technique for monitoring structural integrity in tough materials. If acoustic emission is to be applied to such materials considerable care will need to be exercised to optimise detection techniques, so that low amplitude emissions can be detected against the background noise. This means using narrow bandwidth, highly sensitive piezoelectric transducers which are closely spaced on the structure so as to minimise the effect of signal attenuation. It is also important, as Birchon has reported [1], to choose carefully the observation frequency in order to minimise background interference. These requirements for detectability have, as we shall see in section 5.3 a detrimental effect upon the ability to assess defect significance.

5.2 Locating the Position of Flaws

Details of a number of successful flaw location techniques have been published recently [125, 127-132]. It is clear that if a flaw emits a sufficiently energetic acoustic emission then the position of the flaw

can be estimated by measuring the time delays between detection at an array of transducers covering a structure. However, for accurate location a knowledge is required of, amongst other things, the velocity with which the wave travelled from the source to the transducer. Although wave velocities are well characterised in elastic semi-infinite solids they can often depend upon geometry for the types of engineering structures of interest. The normal procedure is therefore to calibrate the surface wave velocity by pulsing a transducer so that it simulates acoustic emission signals, and then to measure delay times. However, source location by this method is restricted to the approximate position of its epicentre, and no information is recorded which enables the source depth to be measured. One possible, innovatory approach may be to measure the delay in arrival between the longitudinal and shear components of the emission provided they can be detected, since this is proportional to the source to transducer distance as opposed to the epicentre-transducer distance measured for surface waves.

5.3 Assessing the Significance of Flaws

When an acoustic emission signal is detected by a transducer and its position within a structure computed, a judgement has to be made regarding the significance of the event. There are a number of possibilities: did the event come from some flaw which is about to cause structural failure, did it come from an inclusion failure or dislocation motion associated with subcritical crack growth, or was it spurious (eg surface oxide layer cracking)? This question is important because many acoustic emission signals are produced during the testing of a structure, and only a few may be associated with its failure, so that it would be uneconomical to close down a structure each time an event was detected. This is the

problem which at present is proving extremely difficult to solve. One indication of defect severity is given by observing the spatial distribution of events [125], since a number of events clustered at one point may be indicative of a major growing flaw. But this method is unreliable. Two techniques which have been proposed for characterising the severity of a flaw by analysis of the emission waveform are amplitude distribution [12, 133] and spectral frequency analysis [26, 30, 31, 32, 134, 135] discussed previously in Sections 2.4.3 and 2.4.4.

5.3.1 Amplitude Distribution Analysis

It has been shown that for laboratory experiments the amplitude distribution of acoustic emission signals changes as the mode of deformation/fracture changes [99, 100]. When deformation occurs by a few discrete steps a peak is observed at high amplitudes which is absent when the deformation occurs by a large number of small processes. Thus, it is usually argued, measurement of the amplitude distribution on an engineering structure will give a method of determining the mode of flaw growth.

However, the problems with this technique are first that the amplitudes of signals detected with narrow band transducers depend upon the frequency spectrum of the acoustic wave (which can vary from event to event), so that sources of idential strength appear to have different amplitudes, and second that elastic waves detected on the surfaces of engineering structures are subject to attenuations which vary depending upon the source to transducer distance and orientation relationship. These attenuations originate from material attenuation/scattering and geometrical spreading of the elastic waves. In addition, as Pekeris and Lifson [23] have shown, (Section 2.2) the surface wave amplitude even for

a simple point force buried within an infinite half-space can vary because of diffraction effects, and these are particularly important close to the epicentre (when other sources of attenuation are minimised).

5.3.2 Frequency Analysis

Deformation and fracture events have characteristic lifetimes; for instance, the growth of a 30 μm long cleavage microcrack in iron at a velocity of about a tenth the shear wave velocity lasts for ~100 ns. Thus, the elastic waves emanating from the crack will have frequencies extending well above 10 MHz. If, however, the crack length were increased (perhaps by increasing the grain size) so that the crack event lasted longer, one would expect a shift to lower frequency in the energy spectral density function. It has been suggested [31] that different types of acoustic emission source will generate different spectra and that critical flaw growth might be characterised by its spectral "fingerprint". As we saw in Section 2, some success has been claimed for this approach in laboratory tests [26, 31], but it requires the use of broad band (and hence insensitive) transducers combined with relatively simple geometry specimens. For the general case of a complex geometry engineering structure where ambient noise levels require measurements over narrow frequency ranges, convolution of the source function with the transfer functions of the structure and transducer is likely to make it extremely difficult to observe these "fingerprints".

So what should we do to more fully characterise critical flaw growth? The answer is not clear at present because we do not know the relationships between the measured parameters of acoustic emission signals and the dynamic properties of source events. Theoretical and experimental studies at both the National Bureau of Standards and Harwell are aimed at this problem, but to date offer no simple practical solution.

It is becoming evident that optimisation of existing techniques will be inadequate, and an innovatory step is required in this important field.

6. Concluding Remarks

A considerable amount of work in the field of acoustic emission has been published in the scientific and engineering literature of the last twenty years. Whilst we have only been able to include a selection from the literature, we have endeavoured to make this as representative as possible. The review has attempted to emphasise a number of important aspects. Firstly, the basic physical processes involved in the generation, propagation and detection of acoustic emission have been discussed. Secondly, sources of error in existing interpretations of acoustic emissions were highlighted. Thirdly, we have critically discussed the origin of acoustic emission signals during deformation and fracture of metals.

As a consequence of this, a number of recommendations have been made concerning the practical application of aooustic emission; the most significant of these being the use of narrow band, high sensitivity techniques to detect the presence of defects and separate, sophisticated, wide-band techniques to start assessing their significance.

The great majority of laboratory studies have, up to now, been essentially qualitative, mainly because of the use of uncalibrated, poorly defined detection procedures. Facilities now exist for at least partial calibration of detection systems and it is to be hoped that future work will be standardized to facilitate exchange and comparison of the results of different workers. Of equal importance has been the gradual trend toward control and systematic variation of microstructure and testing variables.

Given the task of relating the features of the measured acoustic emission from an experiment, to the properties of the deformation or fracture process by which it is generated, it is now evident that a number of requirements have to be fulfilled.

1. Detection systems must be able to cover the majority of the frequency spectrum of the source. This requires developments at high and low frequencies.
2. Errors in acoustic emission measurements due to instrumentation need to be measured and corrected.
3. A clear understanding of elastic wave propagation in the specimen of interest is required.
4. An adequate theory needs to be developed to allow the interpretation of the properties of an acoustic emission source to be inferred from acoustic emission measurements. Great advances in the interpretation of earthquake seismograms suggest that this is possible for acoustic emission measurements.

Acoustic emission still affords the opportunity to gain an exciting new insight into the dynamic behaviour of deformation events in bulk specimens undergoing deformation and fracture. In addition, because of its passive nature, the monitoring of acoustic emission does not alter the mechanism of deformation. However, for this potential to be fully realised the requirements presented above have to be fulfilled. This has not yet happened and the application of acoustic emission as a NDT technique for monitoring structural integrity of metallic structures has consequently had mixed success to date. However, we feel that acoustic emission will have a role to play in future years in the battery of NDT techniques which may be brought to bear on important engineering problems.

Acknowledgements

We should like to record our appreciation of the many helpful discussions with our colleagues at Harwell during the compilation of this review. In addition, we wish to thank Dr G Clark and Dr J Knott of Cambridge University for the use of their unpublished literature survey.

References

1. D Birchon: British J.N.D.T., 1976, 13(3), 66.
2. H N G Wadley and C B Scruby: Metal Science Journal, 1978, 12(6), 235.
3. D R James and H Carpenter: J Appl Phys, 1971, 42(12), 4685.
4. R Pascual: Scripta Met, 1974, 8, 1461.
5. R T Sedgwick: J Appl Phys, 1968, 39(3), 1728.
6. R M Fisher and J S Lally: Can J Phys, 1967, 45, 1147.
7. N Kiesewetter and P Schiller: Phys Stat Sol (a), 1976, 38, 569.
8. W P Mason: Eng Fract Mech 1976, 8, 89.
9. P P Gillis: Mat Res Stan, 1971, 11(3), 11.
10. P P Gillis: Acoustic Emission, ASTM STP505, 1972, 20.
11. P P Gillis and M A Hamstad: Mat Sci and Eng 1974, 14, 103.
12. A A Pollock: NDT, 1973, Oct 264.
13. M Mirabile: NDT, 1975, April, 77.
14. J D Eshelby: Proc Roy Soc, 1962, 266A, 222.
15. B W Stump and L R Johnson: Bull Seism Soc America, 1977, 67(6), 1489.
16. H Lamb: Phil Trans Roy Soc A, 1903, 203, 1.
17. C L Pekeris: Proc Nat Acad Sci, 1955, 41, 472.
18. C L Pekeris: Proc Nat Acad Sci, 1955, 41, 629.
19. R Burridge and J R Willis: Proc Camb Phil Soc, 1969, 66, 443.
20. J R Willis: Phil Trans Roy Soc A, 1973, 274, 435.
21. J A Simmons and R B Clough: 8th World Conf NDT, 1976, Cannes, France.
22. A Roy: Geophys J R Astr Soc, 1974, 40, 289.
23. C L Pekeris and H Lifson: J.A.S.A., 1957, 29(11), 1233.
24. F R Breckenridge, C E Tschiegg and M Greenspan: J.A.S.A., 1975, 57(3), 626.
25. C B Scruby, J C Collingwood and H N G Wadley: J Phys D, 1978, 11, 2359-2369
26. J Simmons and J R Willis: Unpublished work.

27. A Ceranoglu and Y Pao: Unpublished work.

28. P Fleishman, D Rouby, F Lakestani and J C Baboux: NDT, 1975, Oct, 241.

29. S L McBridge and T S Hutchinson: Can J Phys, 1976, 54(17), 1824.

30. J R Houghton, P F Packman and M A Townsend: 8th World Conf NDT, 1976, Cannes, France, $3K_2$.

31. M Cooper: Phys Bulletin, 1977, Oct 463.

32. R W B Stephens and A A Pollock: J.A.S.A., 1971, 50(3), 904.

33. G J Curtis: NDT, 1974, April, 82.

34. L J Graham and G A Alers: Ultrasonics Symp Proc IEE, Oct 4~7, 1972, 18.

35. K Ono, G Huang and H Hatano: 8th World Conf NDT, 1976, Cannes, France.

36. E R Papadakis: Physical acoustics, 1975, Ed W P Mason, IV(B), New York, Academic Press.

37. E R Papadakis: J.A.S.A., 1965, 37(4), 703.

38. R H Latiff: Ph.D Thesis, Univ Notre Dame, Indiana, 1974.

39. J Speake: Unpublished work.

40. C B Scruby and H N G Wadlet: J Phys. D, 1978, 11, 1487.

41. L Bolin: Bibliograph on AE, Linkoping Univ, Sweden, LITH-IKP R44 196p, 1974.

42. D E W Stone and P F Dingwall: NDT Int, 1977, 10(2), 51.

43. B J Brindley, J Holt and I G Palmer: NDT, 1973, Dec, 299.

44. A A Pollock: Acoustics and Vibration Progress (eds R Stephens and H Leventhall, Chapman & Hall, London), 1974, 51.

45. G J Curtis, NDT, 1975, Oct, 249.

46. R Bracewell: The Fourier Transform and Its Application, McGraw Hill 1965, Chapter 6.

47. K Ono: Mat Eval, 1976, Aug, 1977.

48. A A Pollock: NDT, 1973, 6(5), 223.

49. J V Mullin and R L Mehan: J Testing and Eval, 1973, 1(3), 215.

50. L J Graham and G A Alers: Mat Eval, 1974, Feb, 31.

51. J H Speake and G J Curtis: Int Conf on Carbon Fibres, their place in modern Technology, London, Feb, 1974, Plastics Institution, London, paper 29.

52. K Ono, H Ucisik: Mat Eval, 1976, 35, (2), 32.

53. S P Ying: CRC Critical Rev Sol State Sci, 1973, 4(1), 85.

54. T Imanaka, K Sano and M Shimizu: Bull Japanese Inst Metals, 1973, 12 (12), 871.

55. W P Mason and R N Thurston: 'Physical Acoustics: Principles and Methods', Vol 11, Ch 6, 1975, London, Academic Press.

56. B H Schofield: Acoustic Emission, ASTM STP 505, 1972, 11.

57. H L Dunegan and A T Green: Acoustic Emission, ASTM STP 505, 1972, 100.

58. H L Dunegan and D O Harris: Ultrasonics, 1969, 7, 160.

59. A B L Agarwal, J R Frederick and D L Felback: Met Trans, 1970, 1, 1069.

60. J N Kerawalla: Ph D Thesis, 1965, Univ Michigan.

61. P Jax and J Eisenblater: Battelle, Frankfurt, 1973, Information,15, 2.

62. J Eisenblatter, P Jax and H J Schwalbe: 'The Second Acoustic Emission Symposium', 2-4 Sept, 1974, Tokyo, Japan.

63. T Imanaka, K Sano and M Shimizu: Crystal Lattice Defects, 1973, 4,57.

64. K Kuribayashi, H Tanaka, T Kishi, R Horiuchi and A Kato, Proc 3rd Acoustic Emission Symposium, Tokyo, Japan, Sept 16-18, 1976.

65. B Chalmers and R King: Prog in Metal Phys, 1969, 8, 1.

66. H Hatano: J Appl Phys, 1977, 48(10), 4397.

67. E Siegel: Acta Met, 1977, 25, 383.

68. R Bill: 'Ph D Thesis', 1970, Univ Michigan.

69. T Kishi, H Tanaka and Y Obata: Proc Conf Physical and Metallurgical Aspects of Acoustic Emission, Chelsea College, London 19-21 Dec 1977.

70. P Fleischmann, F Lakestani and J C Baboux: Mat Sci and Eng 1977, 29, 205.

71. H Hatano, N Niwa, T Kishi and R Horiuchi: Hihakai Kensa, 1972, 21,(4), 219.

72. M A Hamstad and A K Mukherkee: UCRL Report 77502, 1975.

73. D R James and S H Carpenter: Scr Met 1976, 10, 779.

74. P Fenici, N Kiesewetter and P Schiller: EUR-5550, c 1974-75, 173.

75. R Bianchetti, M A Hamstad and A K Mukherjee: ECRL Report 77289, 1975.

76. S H Carpenter and F P Higgens: Paper submitted to Met Trans A.

77. H N G Wadley and C B Scruby: 'Fifth Meeting EWGAE', Copenhagen, 1976.

78. R H van Stone, R H Merchant and J R Low: ASTM STP 556, 1974, 93-124.

79. W F Hartman: Exp Mech 1974, 14(1), 19-23.

80. H Hatano: J Appl Phys 1976, 47, No (9), 3873-3876.

81. F P Higgens and S H Carpenter: Acta Met, 1978, 26, 133.

82. K N Tandon and K Tangri: Mat Sci Eng, 1975, 20, 47.

83. M B Bentley and D Birchon: Proc Inst Acoust to be published.

84. J Holt, I G Palmer and D J Goddard: 'Berichte 20th Symposium der Deutschen Gesellschaftfurmetallkunde, Munchen, 1974, 24.

85. T Ingham, A L Stott and A Gowan: Inst J Pres Ves & Piping 1974, 2(1), 31.

86. T Ingham, A L Stott and A Cowan: Inst J Press Ves and Piping, 1975, 3, 267.

87. P G Bentley, D G Dawson, D J Hanley and N Kirby: TRC Report 2917, 1976.

88. J C Radon and A A Pollock, ASTM STP 559, 1974, 15.

89. K Ono and H Ucisik, UCLA-ENG-7514, 1975.

90. I G Palmer: Mat Sci Eng 1973, 11, 227.

91. S P Ying: J Appl Phys, 1975, 46(7), 2882.

92. I G Palmer and P T Heald: Mat Sci Eng, 1973, 11, 181.

93. M N Bassim, D R Hay and J Lanteigne: Mat Eval, 1976, 34(5), 109.

94. W W Gerberich and C E Hartblower: Int J Fract Mech, 1967, 3(3), 185.

95. J C Radon and A A Pollock: Eng Fract Mech, 1972, 4, 295-310.

96. W W Gerberich, D G Atteridge and L F Lessar: Met Trans A, 1975, 6A, 797-801.

97. J D Desai and W W Gerberich: Eng Fract Mech, 1975, 7, 153-165.

98. T Saito and I Uchiyama: Trans Iron & Steel Inst Jap, 1977, 17(3), 121-127.

99. M Arii, H Kashiwaya and T Yanuki: Eng Fract Mech, 1975, 7, 551-556.

transgranular mechanisms, suggesting that individual emission generating

100. G Clark and J F Knott: J Metal Science, 1977, 11(11), 531-536.

101. T Kishi, S Saito, Y Mishima and R Horiuchi: Proc 3rd Acoustic Emission Symposium, Tokyo, Japan, Sept 16-18, 1976.

102. H N G Wadley and C B Scruby: Accepted for publication in Acta Met, 1979.

103. J Q Clayton and J F Knott: Metal Science, 1976, 63.

104. H N G Wadlet, D Furze, C B Scruby and B L Eyre: Accepted for publication in Metal Science Journal, 1979.

105. H L Dunegan and A S Tetelman: Eng Fract Mech, 1971, 2, 387-402.

106. H H Chaskelis, W H Cullen and J M Krafft: ASTM STP 559, 1974, 31-44.

107. C E Hartblower, W W Gerberich and P P Crimmins: Welding J, 1968, 47(1), 1.

108. D G Chakrapant and E N Pugh: Met Trans A, 1975, 6A, 1155.

109. P McIntyre and G Green: British Journal of NDT, 1978, (20) 3, 135.

110. C E Hartblower, C F Morais, W G Rueter and P P Crimmins; Eng Fract Mech, 1973, 5, 765.

111. T M Morton, R M Harrington and J C Bjeletich: Eng Fract Mech 1973, 5, 691.

112. H L Dunegan, D O Harris and A S Tetelman: Mat Eval 1970, 221.

113. O A Shinaishin, M S Darlow and S J Acquaviua: Mat Eval, 1976, 137.

114. J M Carlyle and W R Scott: Experimental Mech, 1976, 16(10), 369.

115. A A Pollock: Ultrasonics, 1968, April, 88.

116. P H Hutton: Mat Eval, 1968, 26, 125.

117. R G Liptai and D O Harris: Mat Res Standards, 1971, Mar, 8.

118. P H Hutton and D L Parry: Mat Res Standards, 1971, Mar, 25.

119. M Arrington and A A Pollock: Ultrasonics Int, 1973, Conf Proc, 188.

120. D O Harris and H L Dunegan: NDT, 1974, June, 137.

121. R W Nichols: Acoustic Emission, Applied Science Publishers, England.

122. E J Burton: J Br Nucl Energy Soc, 1976, July (3), 265.

123. D O Harris: 22nd Int Instrumentation Symposium, May 25-27, 1976, San Diego, California.

124. A A Pollock: Machine Design, 1976, 48(9), 72.

125. A A Pollock and R Waddin: Dunegan Endevco Technical Report De 77-4, Sept, 1974.

126. A C E Sinclair: CEGB Report RD/B/N4066, Oct, 1977.

127. H L Dunegan: Second Int Conf Press Vess Tech Pt II, San Antonio, Texas, Oct, 1973, 625.

128. P G Bentley, D G Dawson and J A Parker: TRG Report 2482(R), 1973.

129. P G Bentley, E J Burton, A Cowan, D G Dawson and T Ingham: Second Int Conf Pres Vess Tech Pt II, San Antonio, Texas, Oct, 1973, 643.

130. D Birchon, R Dukes and J Taylor: ibid, 669.

131. D Birchon, R Dukes and J Taylor: Inst Mech Eng Conf Periodic Inspection Press Vess, London, June 1974, 38.

132. J B Vetrano and W D Jolly: Mat Eval, 1972, 30(1), 9.

133. M P Kelly, D O Harris and A A Pollock: ASTM STP 571, 1975, 221.

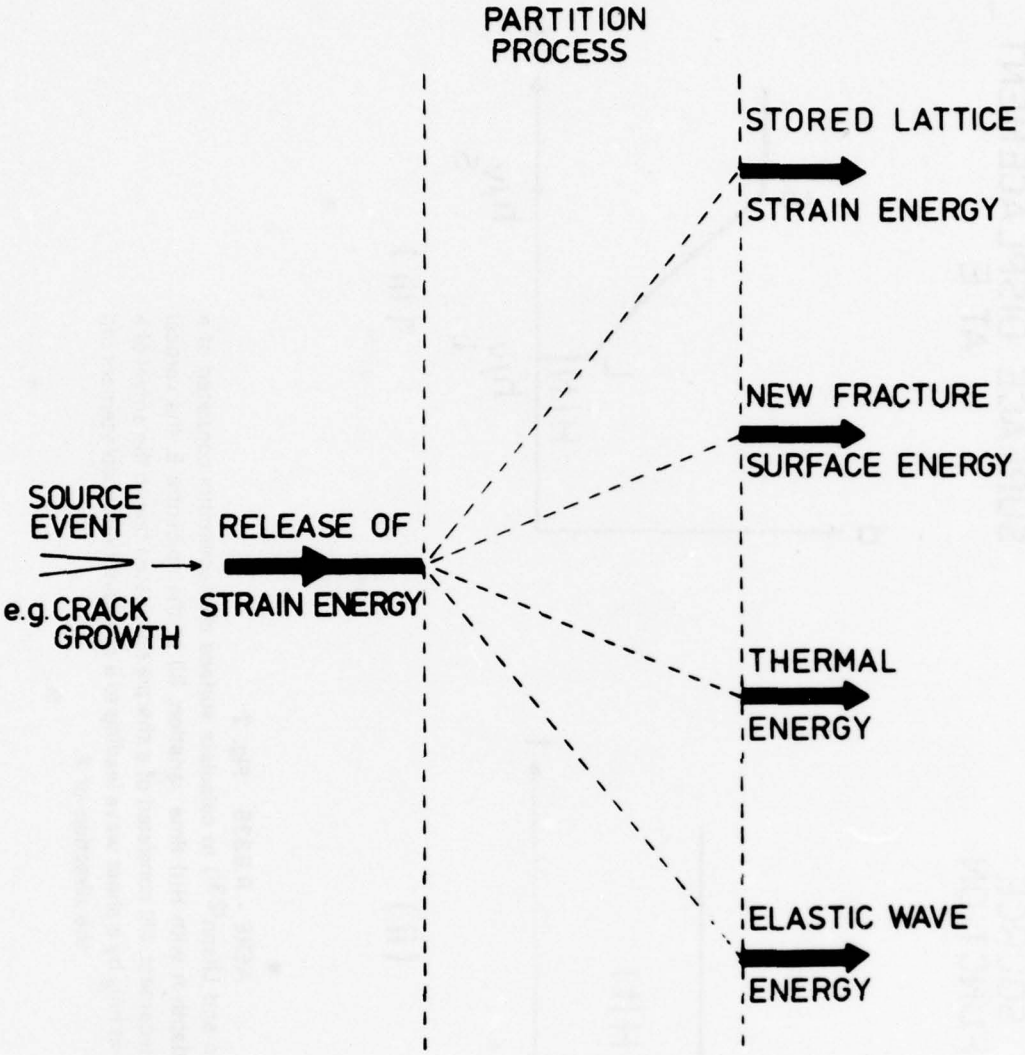

AERE - R.9335 Fig. 1

An illustration of the partition of elastic energy during a crack growth event. The stored elastic strain energy is released in the form of new surface energy, thermal energy and a transient elastic waveform which we call acoustic emission (after Birchon[1]).

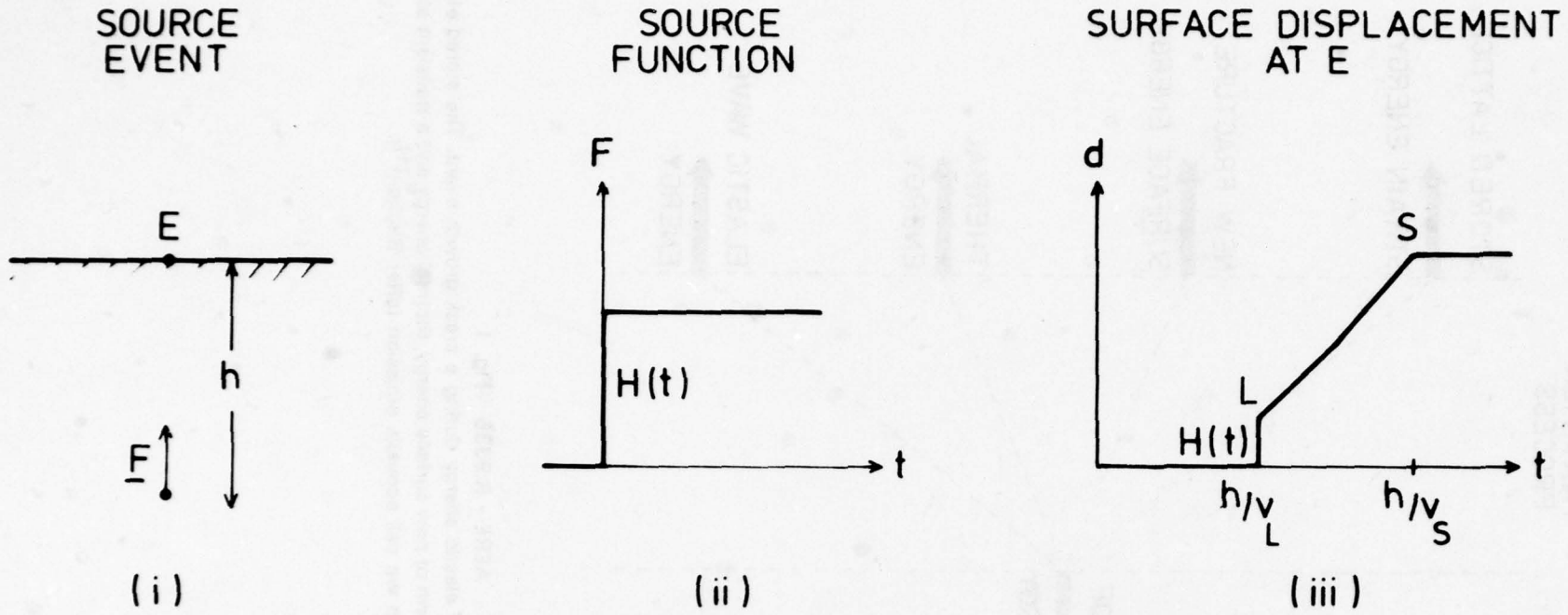

AERE - R.9335 Fig. 2

The model, (i) used by Pekeris and Lifson[23]) to calculate surface displacements consisted of a force monopole at a vertical depth h with H(t) time variation, (ii) at the epicentre E, the vertical component of the surface displacement, (iii) consisted of a sharply rising step due to the arrival of a compressional wave, followed at h/v_s by a shear wave leading to a constant finite displacement ion the direction of F.

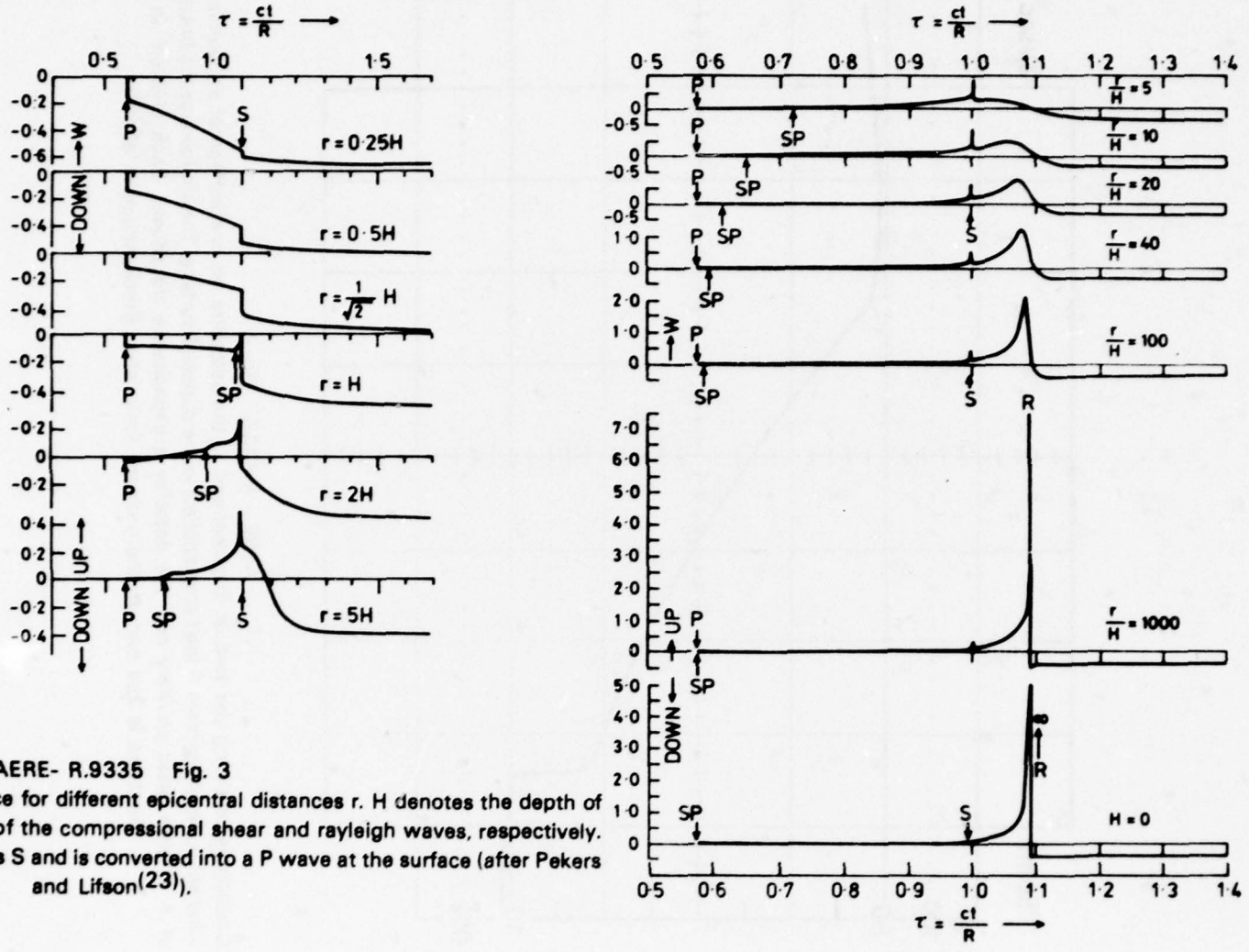

AERE- R.9335 Fig. 3

Vertical displacement W at the surface for different epicentral distances r. H denotes the depth of source. P,S and R denote the arrival of the compressional shear and rayleigh waves, respectively. SP is a diffracted wave which starts as S and is converted into a P wave at the surface (after Pekers and Lifson[23]).

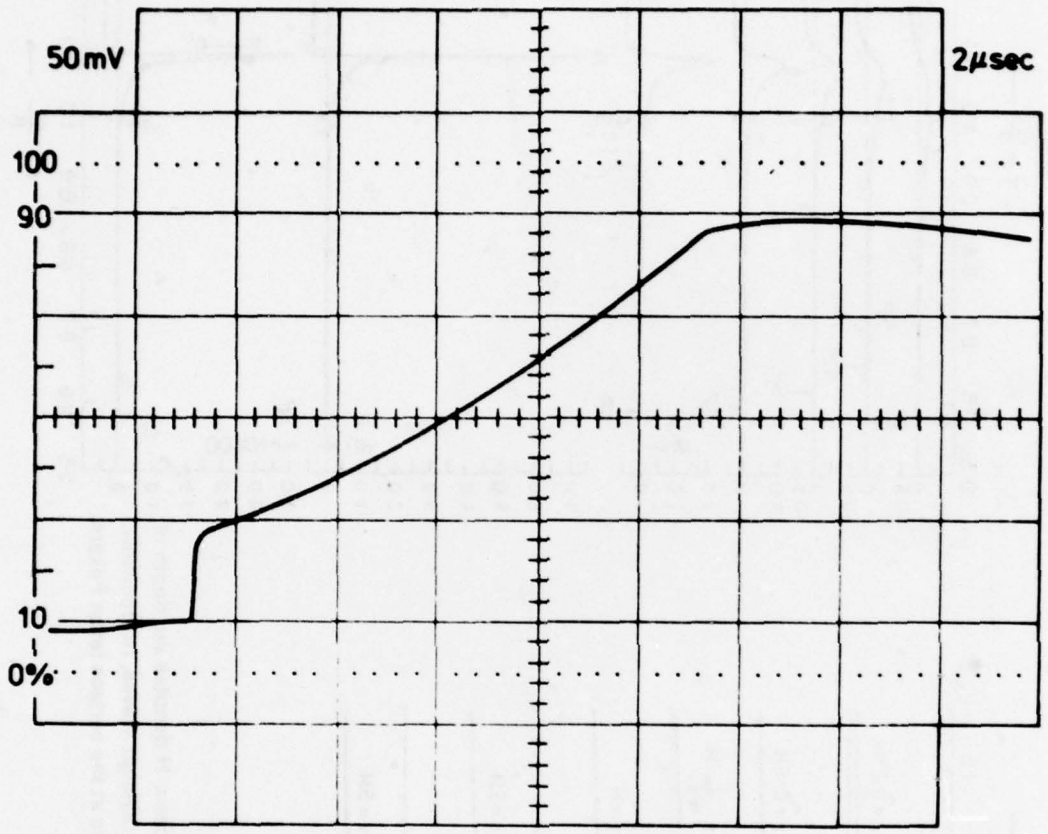

AERE - R.9335 Fig. 4

Oscillogram showing the vertical displacement at the epicentre on one surface of an aluminium alloy block, resulting from A load step applied to the opposite surface. The source was the breaking of A 0.1mm glass capillary and the detector a capacitance transducer. Each division on the Abscissa is 2μs and on the ordinate 5mV (after Breckenridge et al[24]).

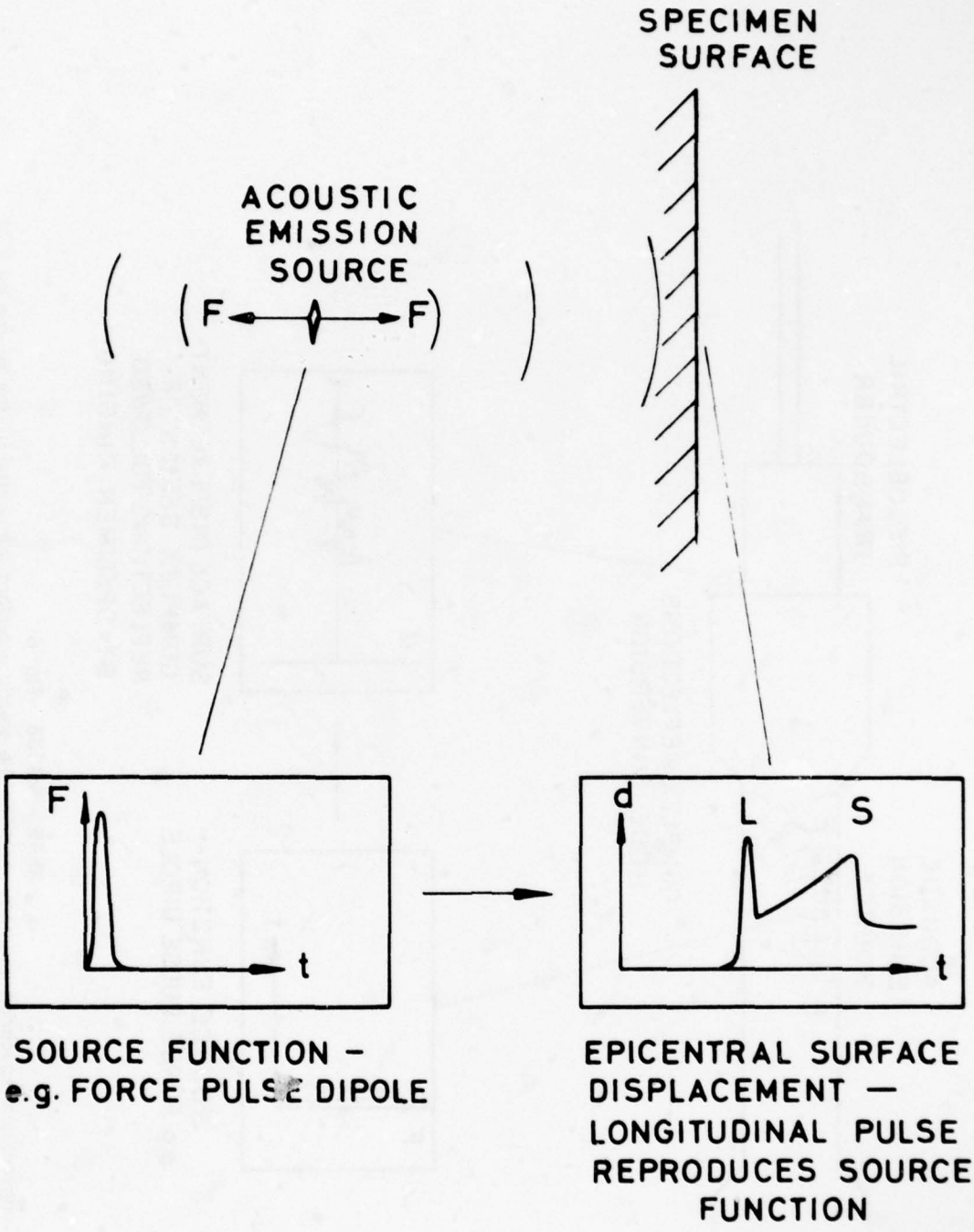

AERE - R.9335 Fig. 5

In semi-infinite specimens, the arrival of elastic waves from the source causes epicentral surface displacements at the epicentre closely related to the source.

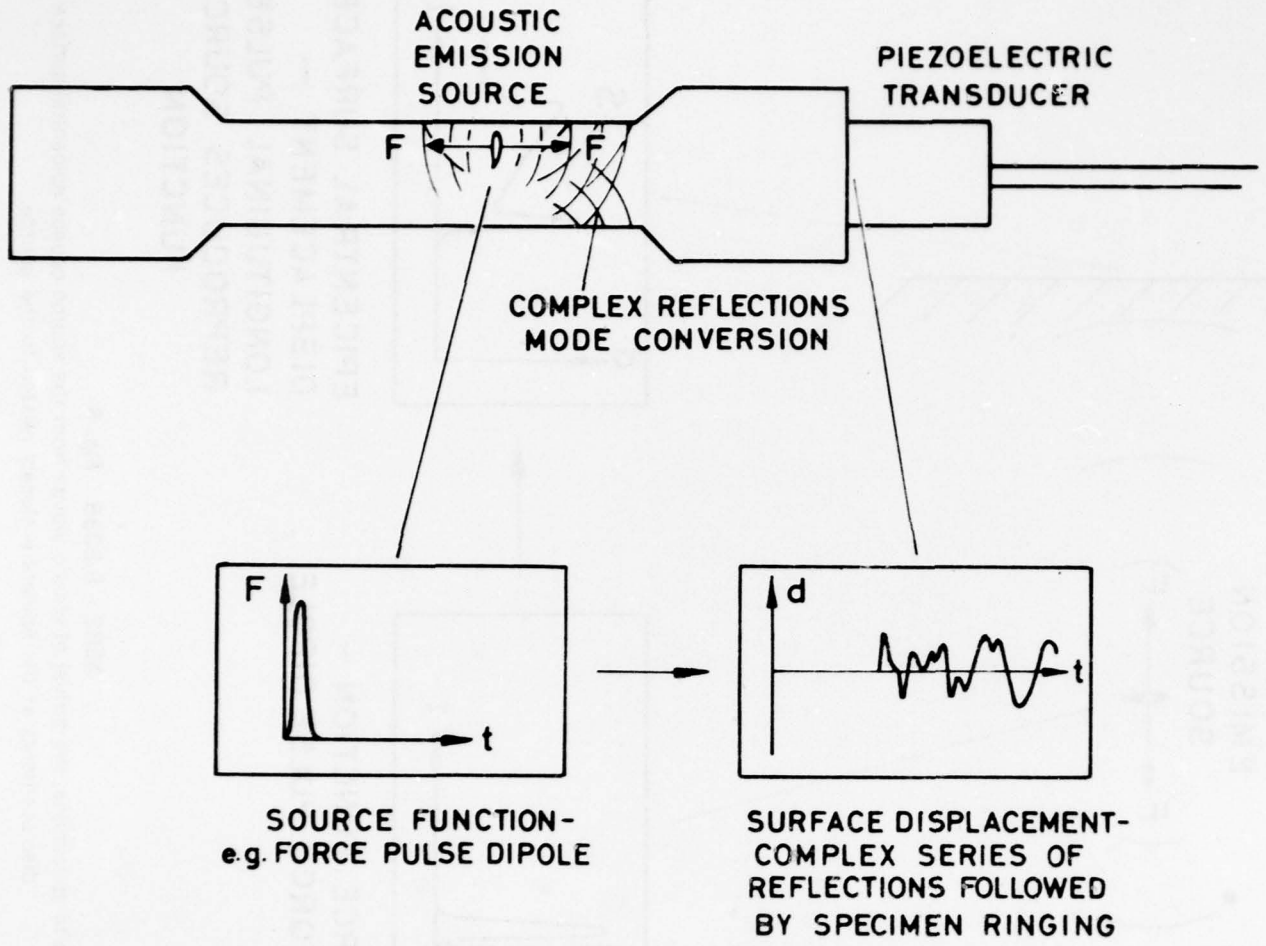

AERE - R.9335 Fig. 6

A conventional specimen geometry modifies the elastic waveform generated by the source by converting energy into the normal modes of the specimen. It is then extremely difficult to recover the original source information.

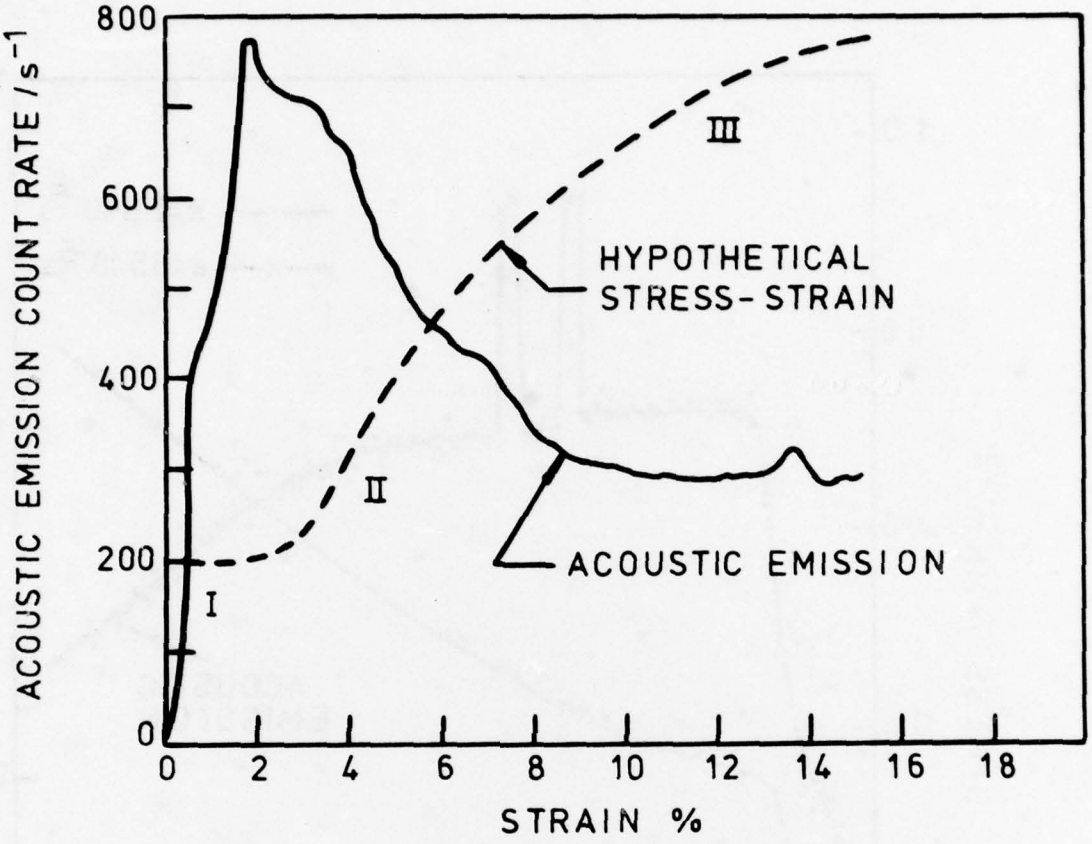

AERE - R.9335 Fig. 7

The dependence of the acoustic emission count rate upon strain for a copper single crystal (from the work of Fisher and Lally[6] reported by Ying[53]).

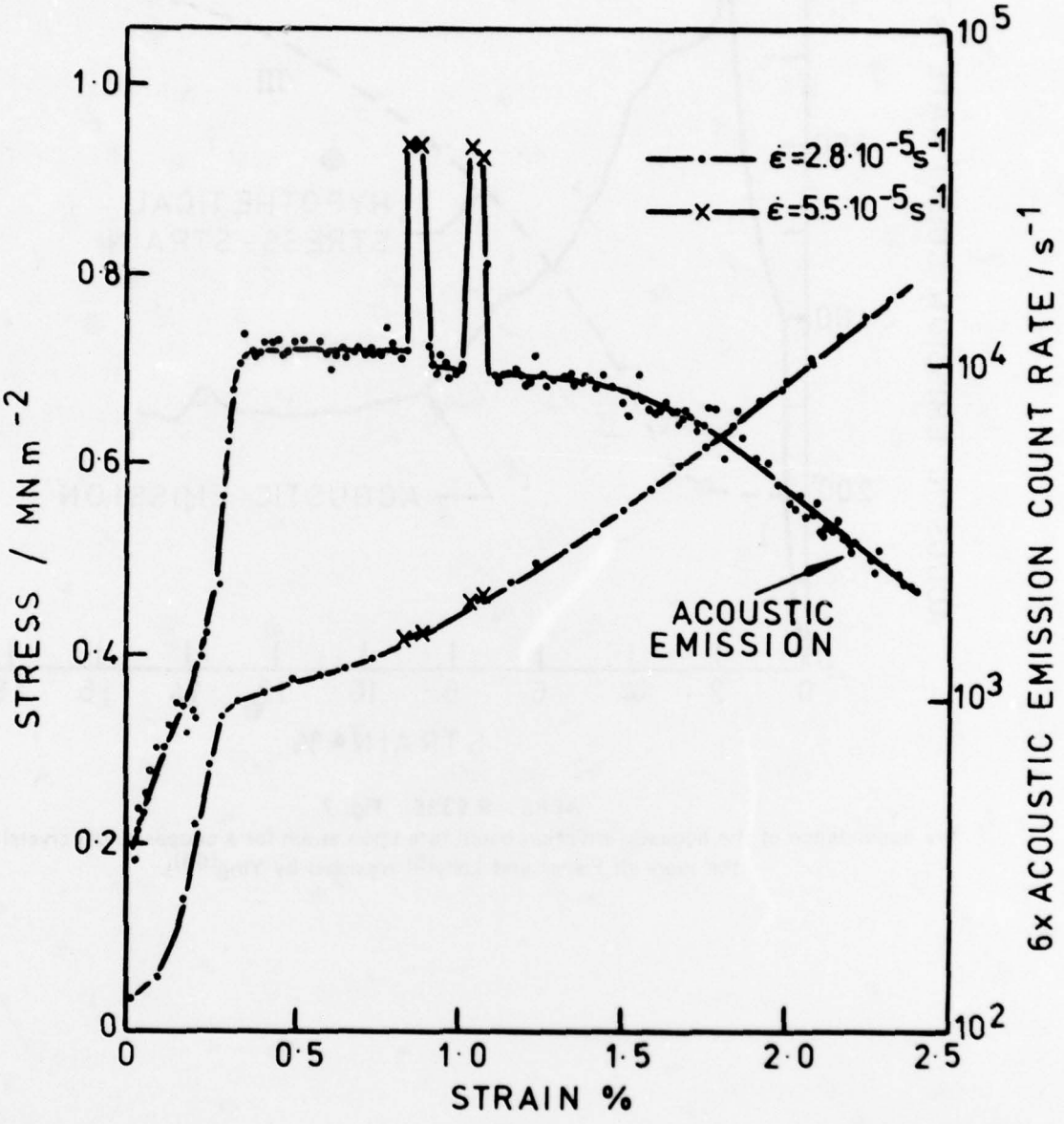

AERE - R.9335 Fig. 8

The dependence of the acoustic emission count rate upon strain and strain rate for a copper crystal oriented for single slip (after Jax et al[61]).

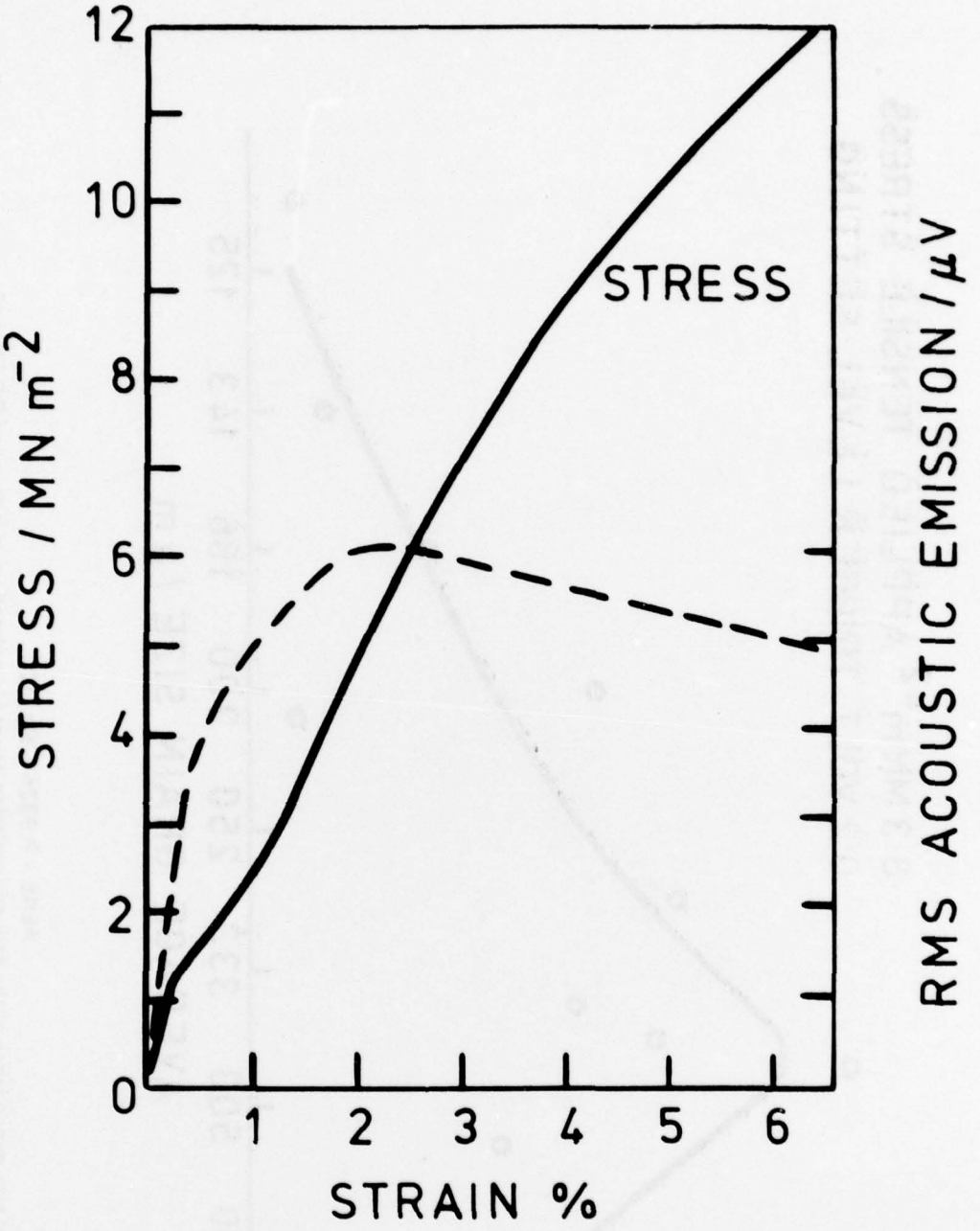

AERE R.9335 Fig. 9

The dependence of the root mean square voltage of acoustic emission signals upon strain from an aluminium single crystal (after Kiesewetter and Schiller[7]).

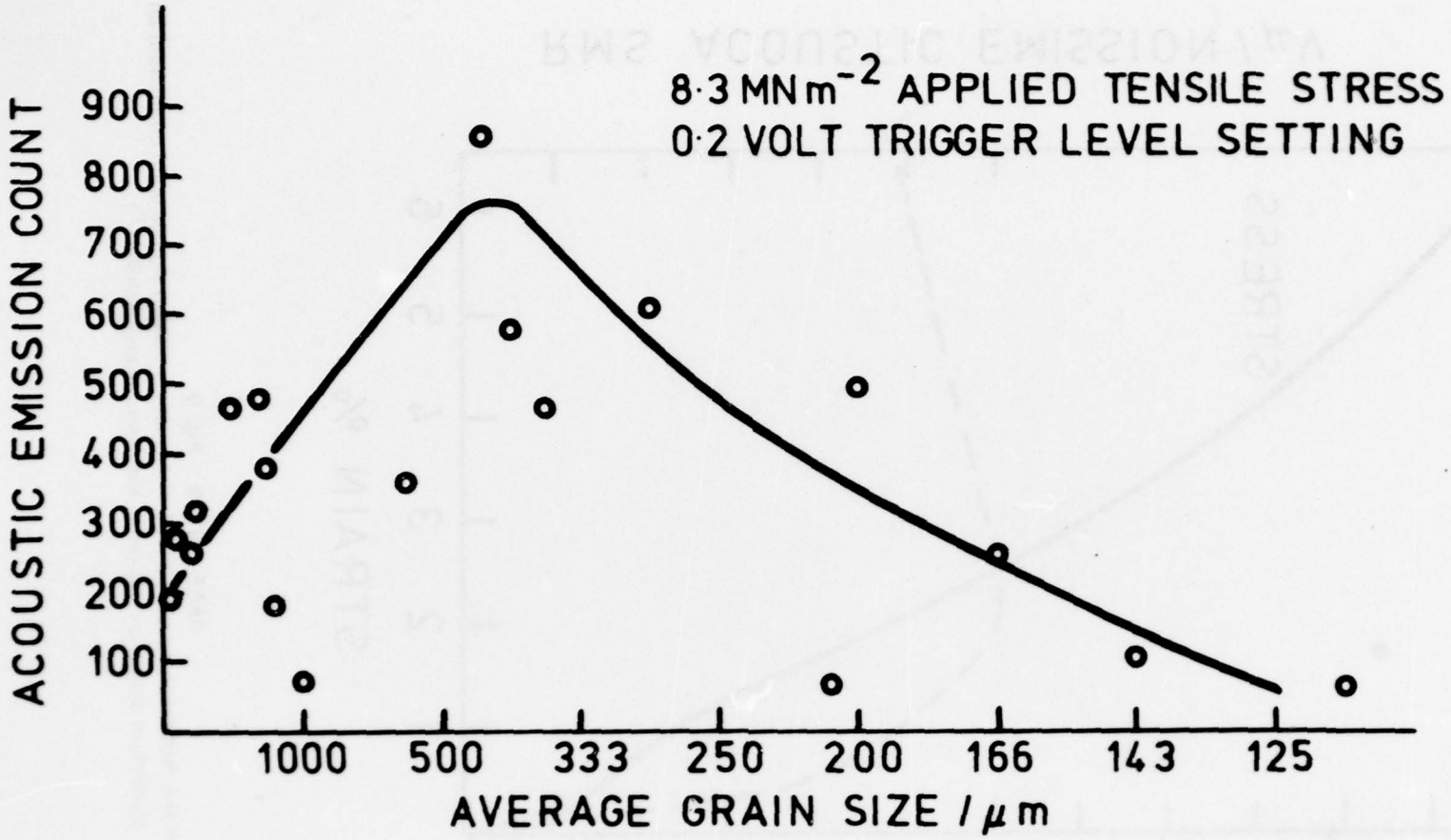

AERE - R.9335 Fig. 10

The grain size dependence of the acoustic emission count (cumulated up to a stress of 8.3 MNm^{-2} for each test) for pure aluminium. Note the reversal of the abscissa (after Bill[68]).

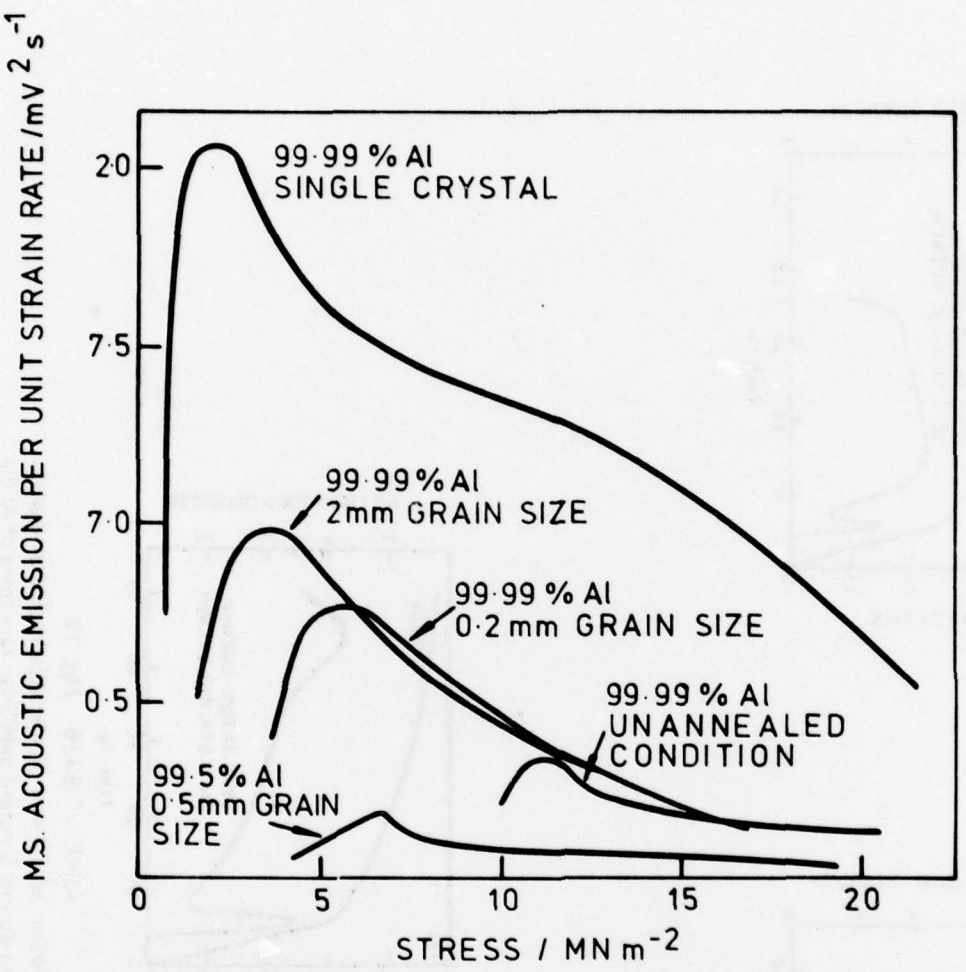

AERE - R.9335 Fig. 11

The stress dependence of the mean square voltage of acoustic emission signals from aluminium specimens with a range of grain sizes (after Kiesewetter and Schiller[7]).

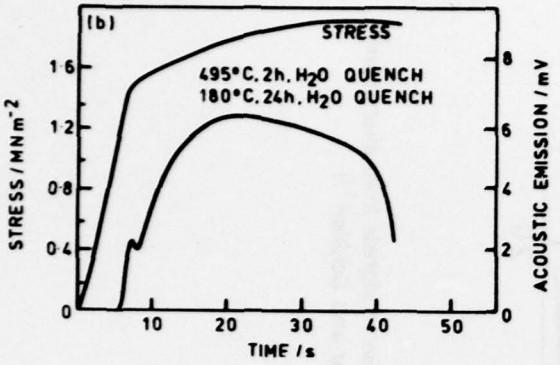

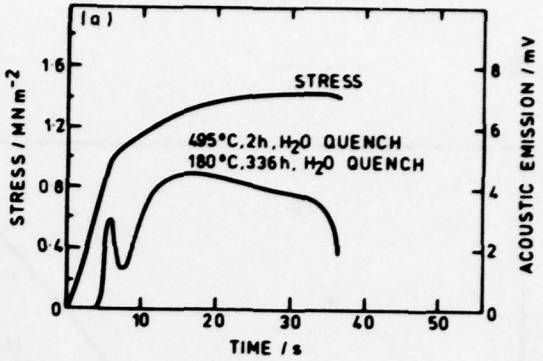

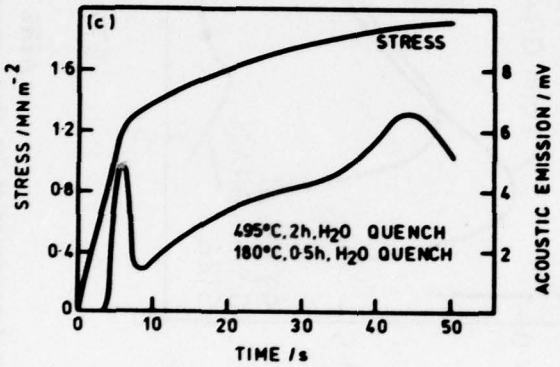

AERE - R.9335 Fig. 12

The variation of voltage of acoustic emission signals with time during constant extension rate tests of Al Cu Mg_2 alloy in three heat-treated conditions (from the work of Zeittler reported by Jax et al[61]).

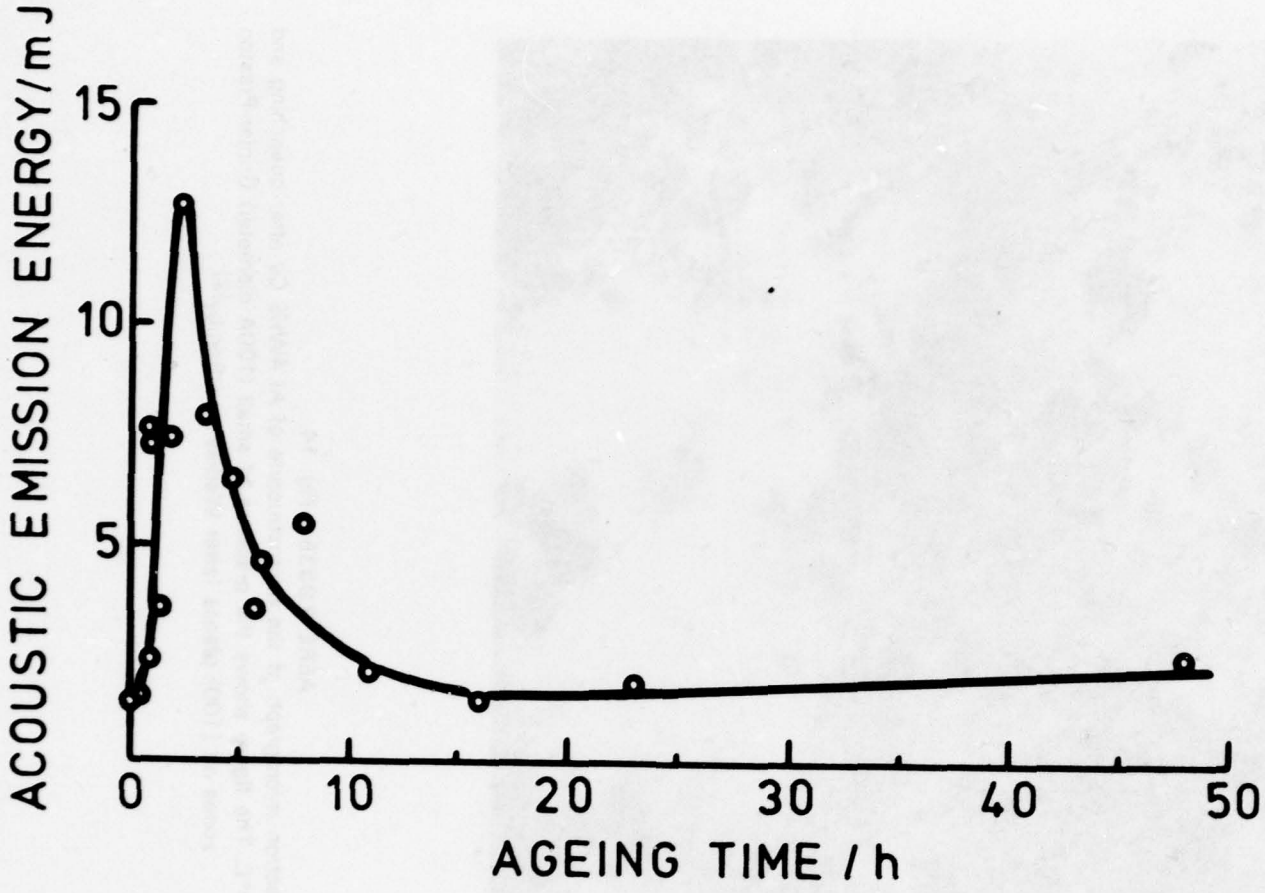

AERE R.9335 Fig. 13

The effect of isothermal tempering at 170°C upon the yield region acoustic emission energy of quenched Al 4Wt% Cu (after Wadley and Scruby[2]).

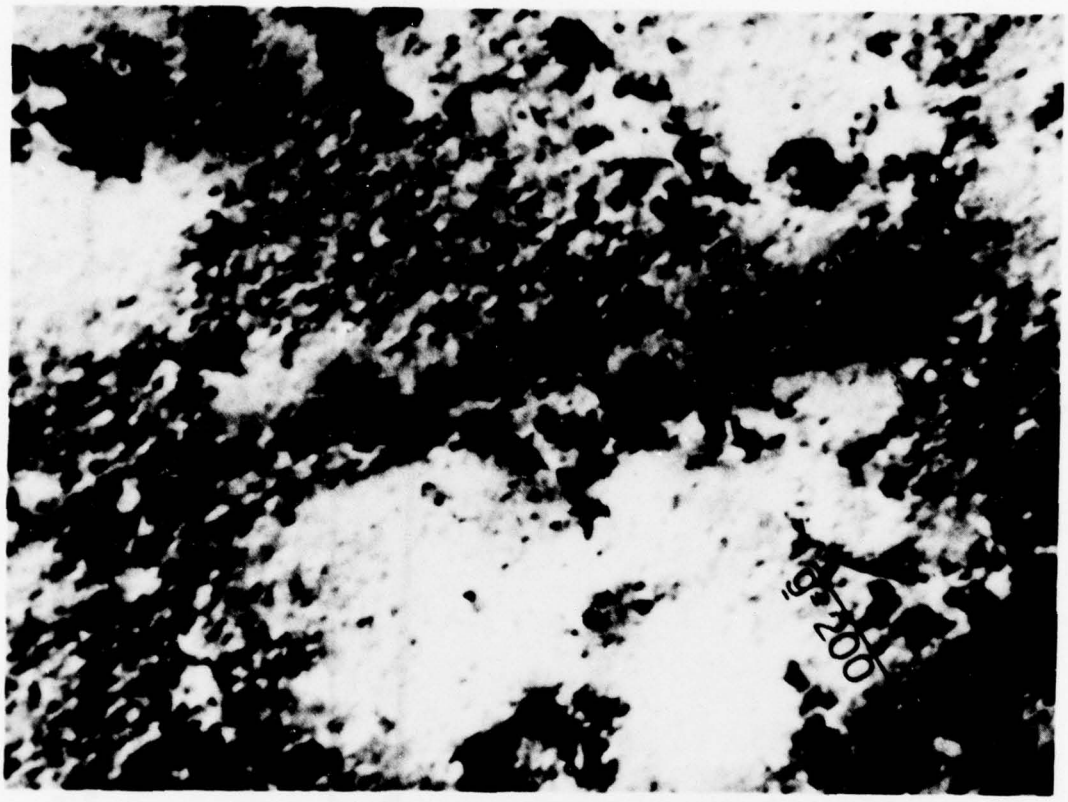

AERE R.9335 Fig. 14

A transmission electron micrograph of the microstructure of Al 4Wt% Cu after quenching and ageing 1h at 170°C. The figure shows the presence of small (100A diameter) Gunier-Preston zones on {100} planes (after Wadley and Scruby[2])

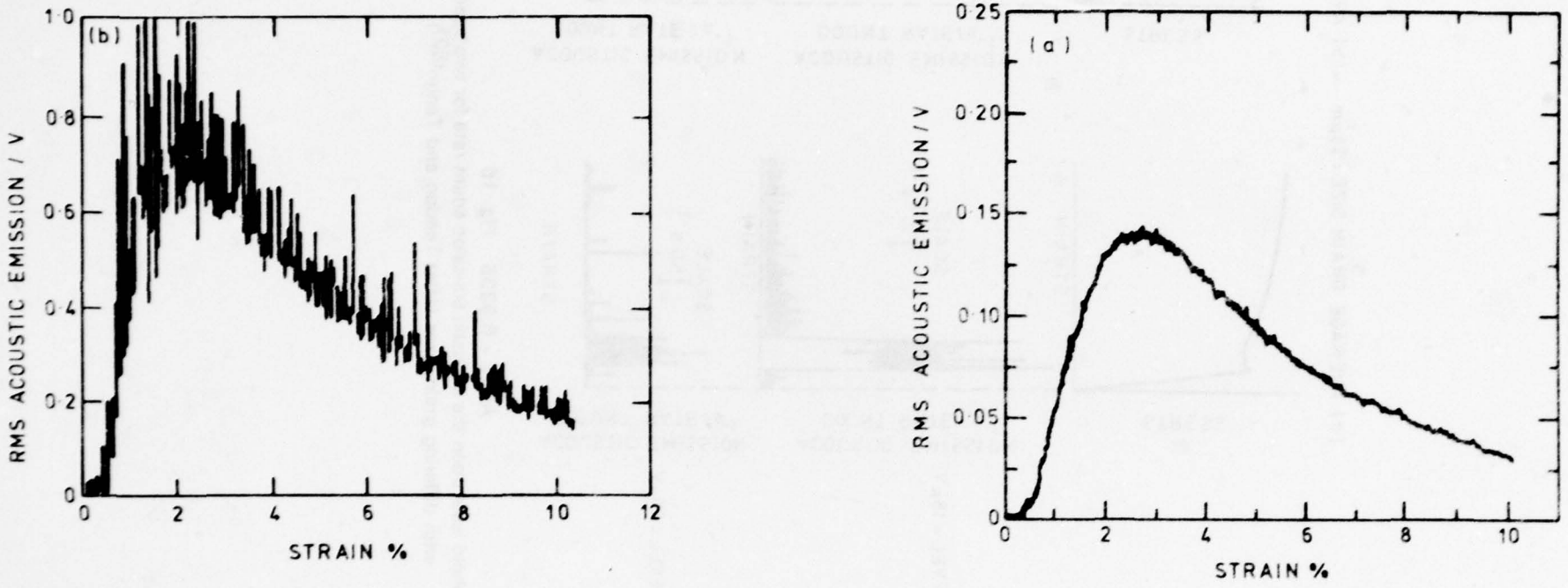

AERE - R.9335 Fig. 15

The dependence of the root mean square voltage of acoustic emission signals upon strain during the deformation of 7075 T6 aluminium (a) one batch of material contained large inclusions and this generated an additional component of burst emissions (b) (75).

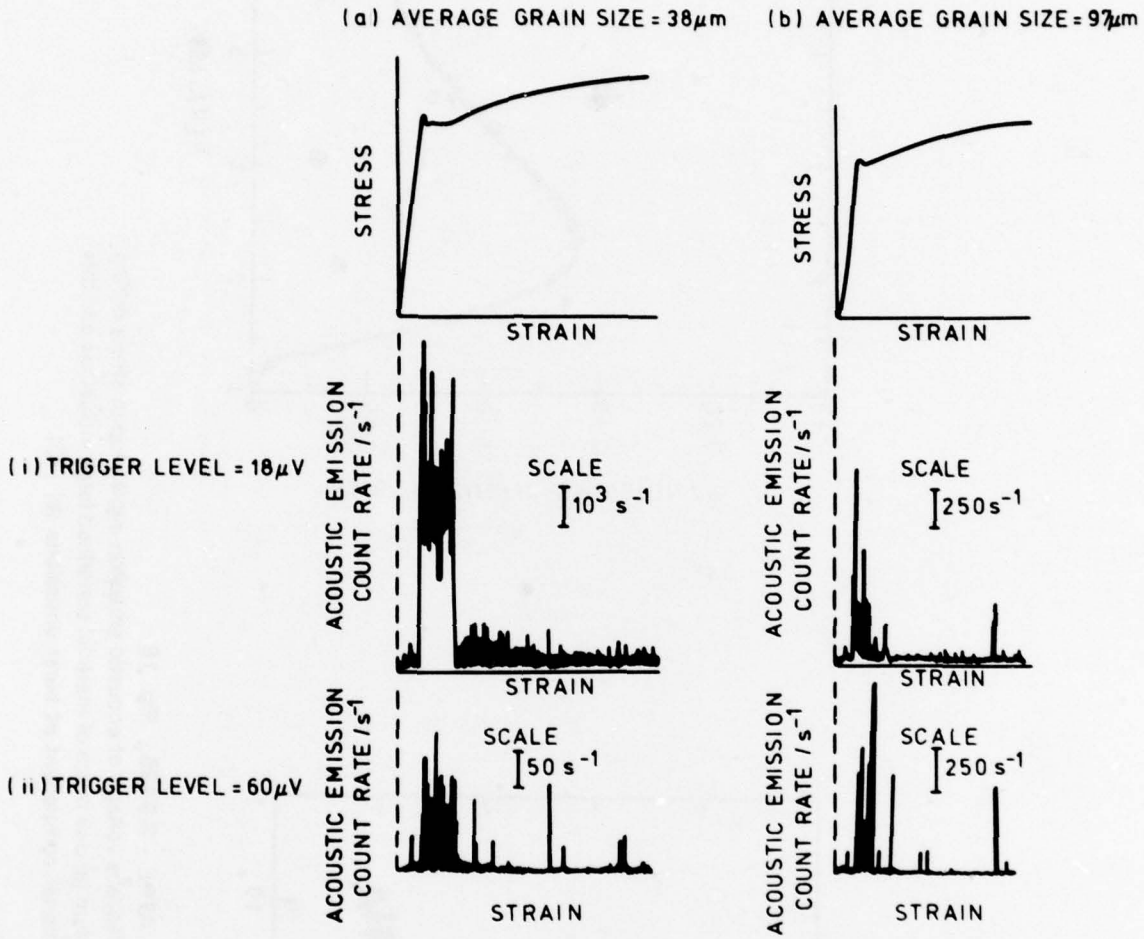

AERE - R.9335 Fig. 16

The effect of threshold level upon the acoustic emission count rate for two specimens of Fe 3% Si with differing grain sizes (after Tandon and Tangri[82]).

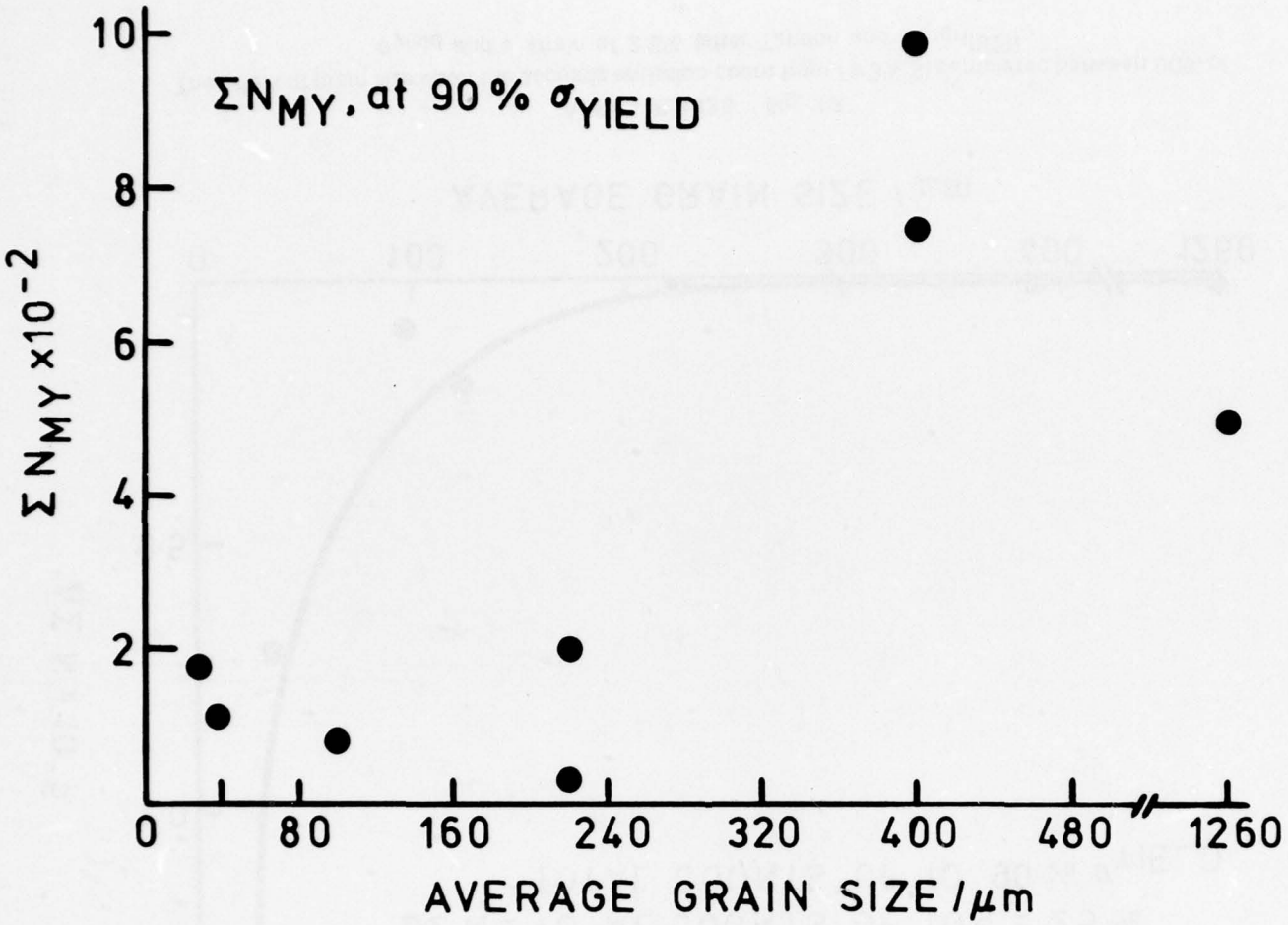

AERE - R.9335 Fig. 17

The effect of grain size upon the acoustic emission count from Fe 3% Si cumulated up to 90% of σ_{yield} (after Tandon and Tangri[92]).

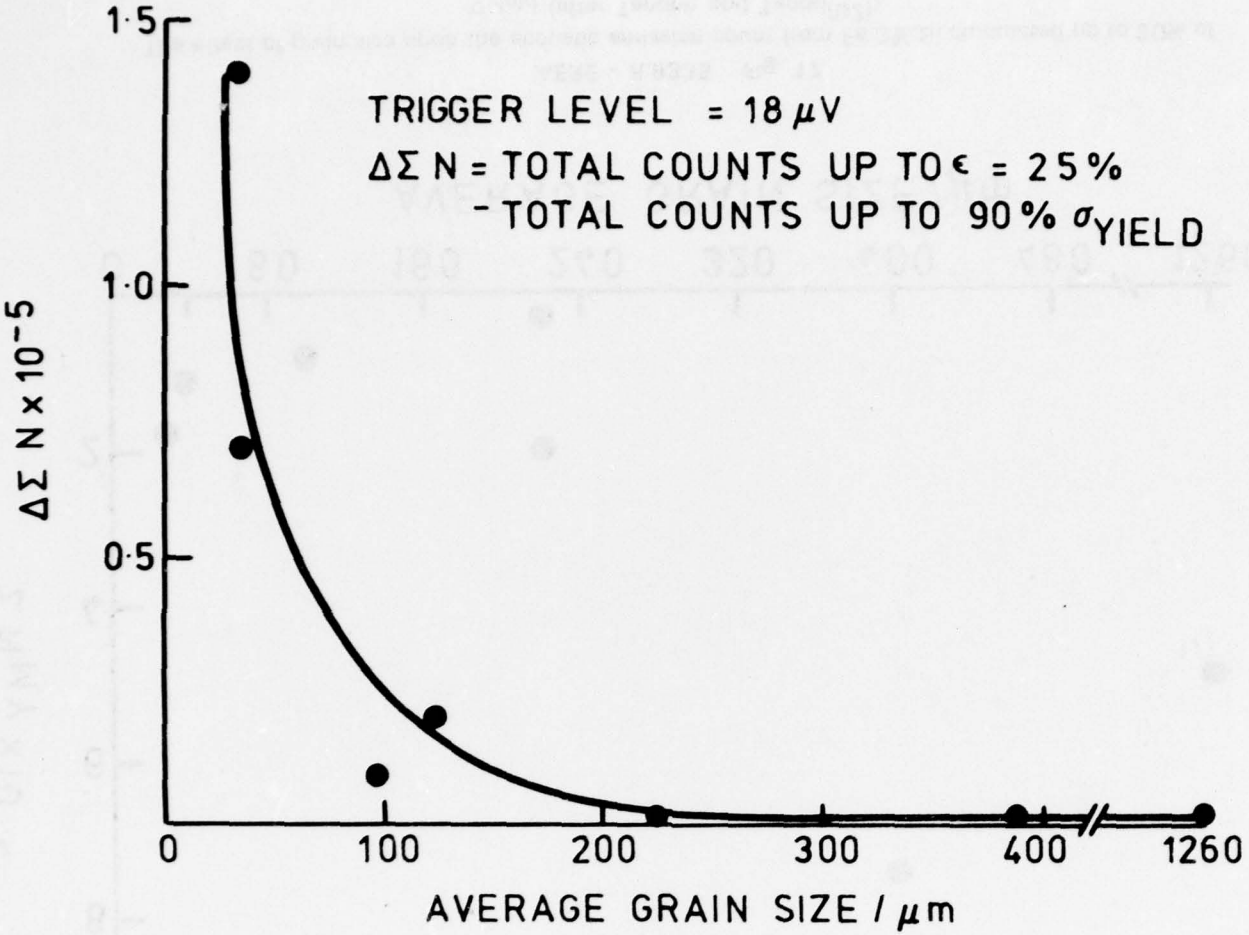

AERE - R.9335 Fig. 18

The effect of grain size upon the acoustic emission count from Fe 3% Si cumulated between 90% of σ_{yield} and a strain of 2.5% (after Tandon and Tangri[82]).

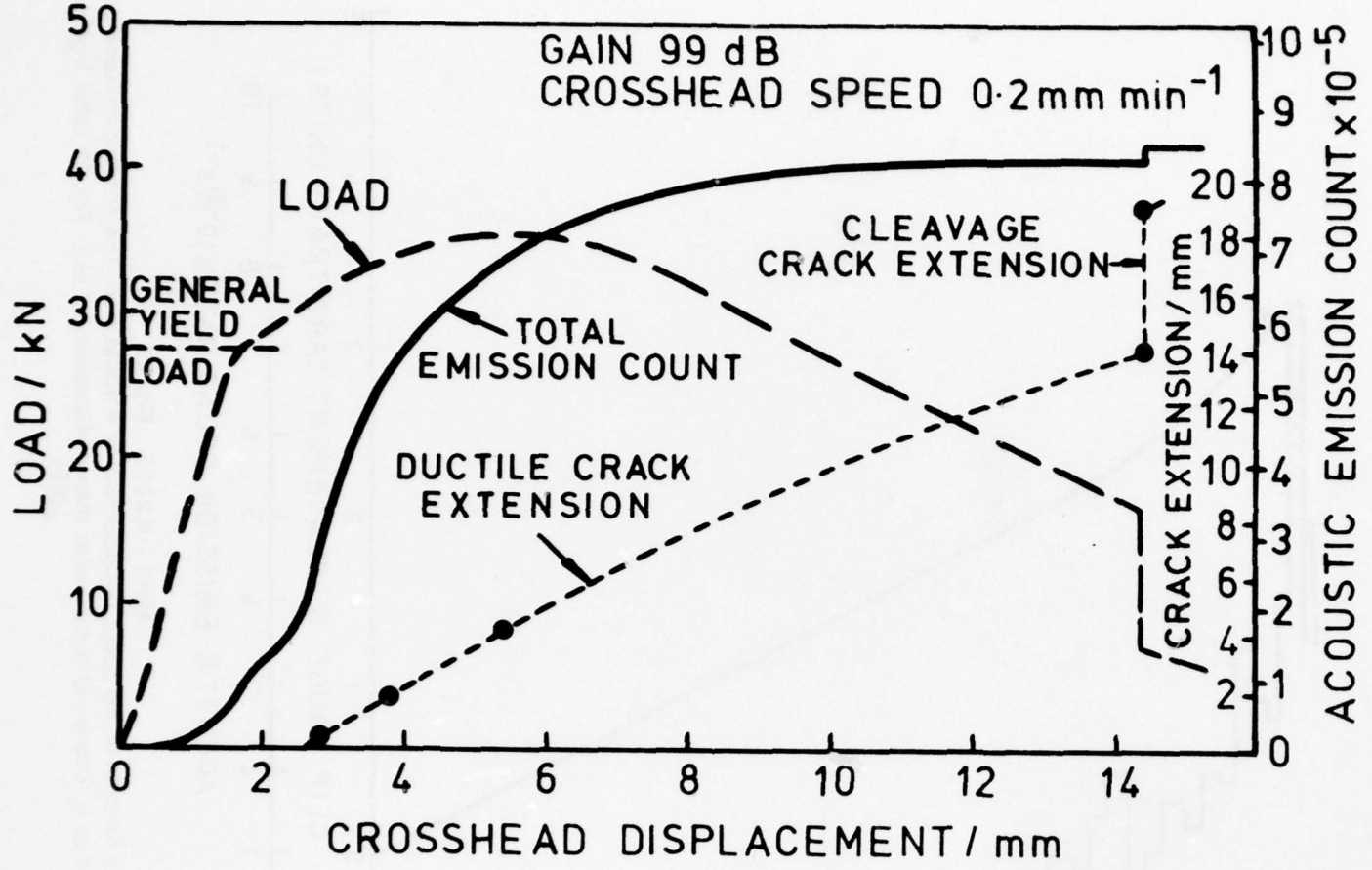

AERE - R.9335 Fig. 19

The total acoustic emission count, load and extension as a function of cross head displacement for a specimen of C/Mn pressure vessel steel pulled to failure at room temperature (after Palmer(90)).

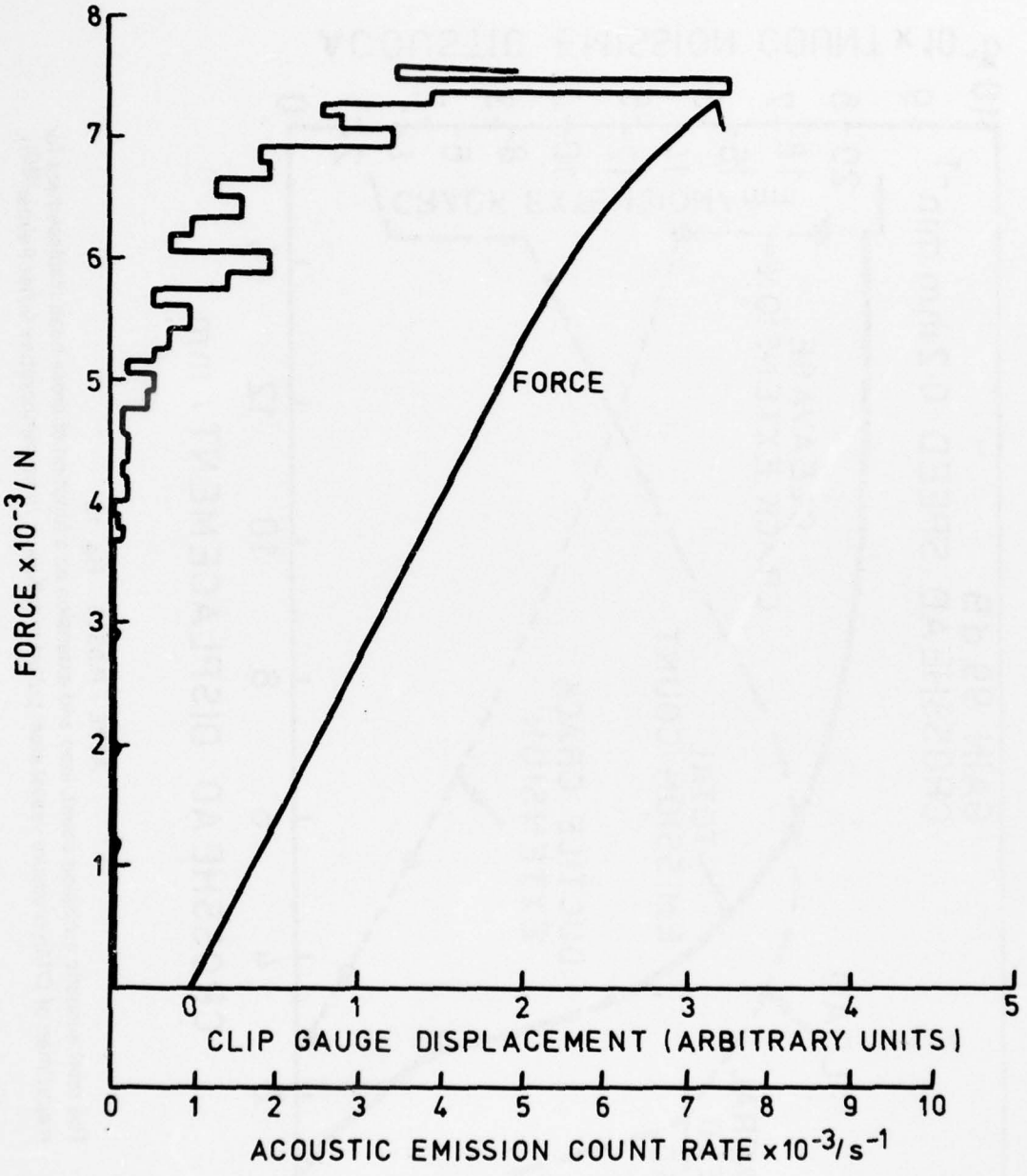

AERE - R.9335 Fig. 20

The force as a function of clip gauge displacement for a 300M steel. The acoustic emission count rate is plotted as a function of force, rather than of displacement as in Fig. 19 (after Ingham *et al*[86]).